Design of a CO_2-based synthesis gas supply chain under demand uncertainty

Mahmutoğulları, Özlem; Mutlu, Nevin; Tan, Tarkan; Pérez-Fortes, Mar

DOI
10.1016/j.compchemeng.2025.109311

Publication date
2025

Document Version
Final published version

Published in
Computers and Chemical Engineering

Computers and Chemical Engineering 202 (2025) 109311

Contents lists available at ScienceDirect

Computers and Chemical Engineering

journal homepage: www.elsevier.com/locate/cace

Design of a CO_2-based synthesis gas supply chain under demand uncertainty

Özlem Mahmutoğulları [a,*], Nevin Mutlu [a], Tarkan Tan [b], Mar Pérez-Fortes [c,1]

[a] School of Industrial Engineering, Eindhoven University of Technology, Eindhoven, The Netherlands
[b] Department of Business Administration, University of Zurich, Zurich, Switzerland
[c] Department of Engineering Systems and Services, Faculty of Technology, Policy and Management, Delft University of Technology, Delft, The Netherlands

ARTICLE INFO

Dataset link: https://edu.nl/bpxfh

Keywords:
Supply chain design
Carbon capture and utilization
CO_2 electrolysis
Multi-period planning
Robust optimization

ABSTRACT

The electrolysis of CO_2 converts CO_2 into value-added products and has the potential to reduce the use of fossil feedstocks by serving as a circular alternative in chemical processes. However, existing literature lacks comprehensive and quantitative analyses of economic, environmental, and governmental factors that can hinder or support its deployment. This study addresses this gap by exploring the potential of CO_2 electrolysis for the production of synthesis gas, syngas, through a supply chain design that integrates long-term decisions on location and infrastructure and medium-term decisions on capacity expansion and aggregate production planning. We identify and quantify time-dependent and uncertain parameters using the Delphi method and employ multi-period planning and robust optimization approaches to consider them, respectively. Moreover, since the environmental impact of syngas is highly dependent on electricity consumption, renewable electricity is utilized with battery support alongside grid electricity. Accordingly, we propose a mixed integer linear programming model to design a supply chain that can serve as a benchmark to make CO_2 electrolysis financially and environmentally viable for syngas production. We conduct a case study on the Benelux region, analyzing different scenarios to derive managerial and design insights. The results show that a design that takes uncertainty into account can reduce syngas production costs by up to 22%. Additionally, although renewable electricity supply variability and different grid characteristics across countries can lead to different strategic decisions with higher costs, increased battery installations and higher government financial support for renewable electricity can help eliminate differences in designs.

1. Introduction

Motivation

Reducing greenhouse gas emissions demands significant efforts from industrialized countries. To meet the Paris Agreement targets, Europe has set a goal to be climate neutral by 2050 (European Council, 2024). Achieving this goal will require the adoption of new promising technologies, as currently widely used technologies still rely heavily on fossil fuels as carbon sources. One promising approach involves capturing carbon dioxide (CO_2) either directly from the air (DAC) or from the flue gases of point sources. Once captured, CO_2 can be stored through carbon capture storage (CCS) or utilized through carbon capture utilization (CCU) technologies. CCU focuses on converting CO_2 into valuable products that replace fossil-based alternatives, offering an option to defossilize (part of) the process industry (IRENA, 2024), especially the chemical industry where the carbon molecule from fossil fuels can be replaced by carbon from CO_2.

The electrochemical reduction of CO_2 (CO_2E) arises in the context of CCU with the potential to produce chemicals and fuels by using CO_2, H_2O, and electricity. This approach not only supports the transition to a more sustainable chemical industry but also enhances the energy independence of the European chemical industry. By electrifying chemical processes and utilizing CO_2, Europe can reduce its reliance on imported fossil fuels (European Parliment, 2023a).

While CCU technologies offer advantages in producing non-fossil-based chemicals and synthetic fuels while reducing dependence on fossil fuels, they also present challenges. These include the efficiency and scalability of CO_2 capture and conversion processes, the need for substantial infrastructure investments, uncertainties in market demand, and the critical role of supportive government policies and incentives to ensure timely development and adoption (Zhao et al., 2023). Addressing these challenges is essential in the design of supply chains. However, the current literature on supply chain design in the context of CCU is scarce. Moreover, as CCU technologies are still developing,

* Corresponding author.
E-mail addresses: o.mahmutogullari@tue.nl (Ö. Mahmutoğulları), m.d.m.perez-fortes@tudelft.nl (M. Pérez-Fortes).
[1] Project coordinator.

https://doi.org/10.1016/j.compchemeng.2025.109311
Received 12 May 2025; Received in revised form 8 July 2025; Accepted 23 July 2025
Available online 5 August 2025

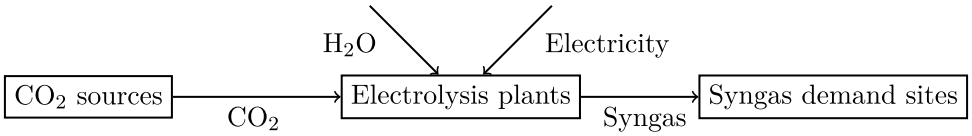

Fig. 1. CO_2-based syngas supply chain network.

it is important to consider the uncertain nature of their supply chain designs. Since a supply chain design involves many interconnected decisions, uncertainties at one level can significantly impact the entire planning process. For example, the uncertainty in CO_2 or electricity supply can disrupt production planning and transportation scheduling; the uncertainty in market demand for CO_2-based products can lead to over or under investment in production capacity; the uncertainty in policies and regulations can directly affect financial considerations or consumer acceptance. In light of this, incorporating uncertainty into supply chain design is crucial to ensure both effectiveness and resilience.

This work focuses on the production of synthesis gas, or syngas, via CO_2E and explores the design of a CO_2-based syngas supply chain. Syngas is a mixture of carbon monoxide (CO) and hydrogen (H_2) and serves as a chemical building block for many products such as hydrocarbons and fuels (Khosravani et al., 2023). Currently, syngas is mainly produced on-site through steam methane reforming using natural gas as feedstock (IEAGHG Technical Report, 2023). Since CO_2E is an alternative to steam methane reforming, the adoption of CO_2E has great potential to reduce the net CO_2 emissions of the chemical industry and other related sectors, such as transportation. However, realizing this potential requires more than just technological innovation because it also demands a well-designed and coordinated supply chain that ensures cost efficiency, scalability, and reliability. Additionally, given the high capital and operating costs, it is essential to have a centralized and optimized design. Such a design should integrate production and distribution systems, incorporate financial support mechanisms, and identify potential bottlenecks. Furthermore, governance plays a crucial role in shaping the viability of this transition because policies and financial incentives directly influence investment decisions, market competitiveness, and the long-term economic and environmental feasibility of CO_2-based syngas production.

We present a case study for the CO_2-based syngas supply chain design considering uncertainty, including economic, environmental, and governance aspects, and providing insights into the necessary conditions for the deployment of CO_2E at scale for Benelux countries (Belgium, the Netherlands, and Luxembourg). We explore how the supply chain design is affected by various scenarios, which are defined by different grid characteristics and renewable electricity transmission rules, and various parameter settings, such as different financial support for capital and operational expenses, operating hours of electrolysis plants, and variability levels of renewable electricity.

Case study

A supply chain network is a multilayer network where the layers generally represent (i) suppliers, (ii) facilities like plants and warehouses, and (iii) customers. As depicted in Fig. 1, we consider a supply chain network consisting of CO_2 sources where CO_2 is captured, electrolysis plants where the electrochemical reduction of CO_2 takes place, as in the chemical Eq. (1) (Hou et al., 2024), and syngas demand sites where syngas is consumed. The figure also shows the inlet water and electricity streams and CO_2 and CO_2-based syngas flows that may come/go to different sites.

$$H_2O + CO_2 \xrightarrow[\text{Electrolysis}]{} H_2 + CO + O_2 \quad (1)$$

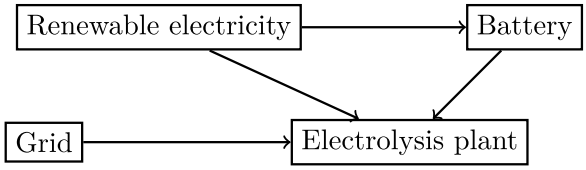

Fig. 2. The proposed electricity consumption system at electrolysis plants.

Electrolysis is inherently energy-intensive, leading to a high demand for electricity. Hence, the global warming potential of CO_2-based syngas is largely determined by the carbon footprint of the electricity consumed during production (Nishikawa et al., 2023; Bachmann et al., 2023). Electricity may be provided by the grid or by exclusive renewable plants. While connecting electrolyzers only to the grid allows continuous electrolyzer operation, it is currently not preferable due to the low share of renewables in the grid, e.g., only 41% for European Union countries in 2022 (Eurostat, 2023a,b). Alternatively, investments can be made in renewable electricity sources, such as solar or wind, for exclusive use by electrolyzers. Although this option is environmentally ideal, the variability in electricity supply can interrupt continuous operation, leading to reduced performance and higher degradation of electrolyzers (Kojima et al., 2023). To address these issues, an integrated approach can be adopted – using electricity from both renewable sources and the grid. Additionally, electricity storage systems can enhance the use of renewable electricity by storing the excess supply for later use (Tebibel, 2021; Li et al., 2023a). Accordingly, this case study considers an electricity consumption system based on the coordinated use of the grid, renewable electricity generation plants, and batteries (see Fig. 2), with corresponding investments in renewable electricity and storage included in the supply chain design.

The price and environmental competitiveness of CO_2-based syngas depend heavily on supply chain design decisions, such as the location and capacity of electrolysis plants, CO_2 and syngas transport infrastructure, and the sizing of renewable electricity and battery systems. Hence, it is essential to design the supply chain considering both financial and environmental concerns. For better consideration of these concerns, we take into account the time-dependency and uncertainty of parameters during the decision-making process. Accordingly, we adopt a multi-period planning approach to reflect changes over time and incorporate the pricing decision of CO_2-based syngas to ensure economic feasibility while meeting carbon footprint targets. To have a design that is immune to the syngas demand uncertainty, we employ a robust optimization approach and define interval uncertainty sets for syngas demand realizations, where sets are dependent on the chosen price.

In this work, a robust optimization approach is used instead of a stochastic optimization approach for three main reasons. First, while handling the uncertainty, robust optimization can provide higher computational efficiency because stochastic optimization often necessitates solving large-scale scenario-based models that can become intractable for complex multi-period supply chain decisions. Second, robust optimization does not rely on precise probabilistic information, making it suitable for our context where historical data is lacking due to the absence of a merchant market for syngas. Third, it offers worst-case

guarantees, ensuring feasible and cost-effective designs under uncertainty, especially vital for long-term strategic decisions such as facility location and infrastructure investments.

We propose a mixed integer linear programming model to solve the robust multi-period supply chain design problem by linearizing nonlinearities caused by the uncertainty and interdependencies between decisions. Over the planning horizon, the following decisions are made: electrolysis plant locations, capacities of plants, batteries, and renewables, the infrastructure for CO_2 and syngas transportation, the product price, served demand sites, capacity expansions for electrolysis plants, batteries, and renewables, delivery amounts of CO_2 and syngas, syngas production amounts, and amounts of grid electricity and renewable electricity – including direct and battery usage – consumed during syngas production. Long-term decisions related to location, initial capacity installations, and transportation infrastructure are made at the beginning of the planning horizon. Medium-term decisions related to capacity expansions are made at the beginning of each period, and short-term decisions related to production planning and electricity consumption can be made multiple times within each period. Our case study considers the Benelux region over a 20-year horizon, divided into four 5-year periods, and short-term decisions are made annually. In a period, short-term decisions and their associated costs occur five times. The cost analysis accounts for the time value of money by calculating the present value of annual costs.

The proposed model aims to ensure both economic and environmental feasibility. To this end, the proposed model respects the targeted carbon footprint level for electricity consumption through constraints. Additionally, the objective function maximizes the total profit to simultaneously support the deployment of CO_2-based syngas for consumers and provide economic incentives for investors to invest in the technology for its future development.

Contributions to the literature

The contributions of this paper can be evaluated from the case study and methodological perspectives. In this section, we review the existing studies that form the basis of our study and highlight the key differences and novel aspects of our work.

First, to the best of our knowledge, this work is the first to consider a multi-period planning approach for the supply chain design of a product produced based on a CCU technology where the uncertainty is taken into account in the decision-making process. A review of existing studies in the context of supply chain optimization for CCU technologies shows that the majority of them deal with design decisions related to CO_2 capture and its distribution to storage or utilization sites, but they lack consideration of utilization processes or transportation of final products. Hasan et al. (2014) present the first work to design a cost-efficient supply chain with a special focus on the costs of using different technologies and materials for carbon capture from point sources. Zhang et al. (2018) extend this work by considering intermediate nodes between CO_2 capture and storage and utilization sites to reduce overall transportation cost by reducing the total length of pipelines. A connected supply chain design for European countries is proposed by d'Amore et al. (2021), where the authors analyze the effects of different scales in capture and transportation costs. Zhang et al. (2020) consider both environmental and financial concerns while minimizing the carbon footprint of the electricity consumed at the stages of CO_2 capture, transportation, and injection. Unlike the mentioned works, Wiltink et al. (2023) consider the transportation of final products and examine how centralized versus decentralized plant location strategies affect the design of a CO_2-based syngas supply chain for Europe. However, none of these works consider the time-dependency and uncertainty of the parameters.

Second, to the best of our knowledge, this work is the first to incorporate an integrated electricity supply including grid, renewable sources, and battery at electrolysis plants into the supply chain design decision-making process to mitigate the drawbacks of the renewable electricity supply variability. Although Wolff et al. (2023) propose a multi-period planning approach for supply chain designs of renewable fuels – produced via various technologies, including CCU – and incorporate investments in renewable electricity sources by considering their capacity and seasonal intermittency, they do not explore the effects of combining grid electricity and battery storage with renewable sources. A system that supports the renewable electricity usage with batteries at water electrolyzers is proposed by Tebibel (2021) and Li et al. (2023a). However, these studies fall within the scope of production planning rather than supply chain management, where production planning is only one component, and also neglect the potential use of grid electricity in the system.

Third, to the best of our knowledge, this work is the first to consider the price-dependent demand uncertainty in the supply chain design, where the price is a decision variable. In the broader literature on supply chain design under uncertainty, demand uncertainty is mostly studied, where most of these studies employ a stochastic optimization approach while a few of them employ a robust optimization approach (Govindan et al., 2017). The works on robust supply chain designs can be categorized according to how the uncertainty realization is defined. While Peng et al. (2011) and Ramezani et al. (2013) consider scenarios for demand realizations, Zokaee et al. (2017) and Keyvanshokooh et al. (2016) consider uncertainty sets that define realizations due to, as stated by Zokaee et al. (2017), challenges associated with defining scenarios accurately and solving models if the number of scenarios is large. Zokaee et al. (2017) employ the robust optimization with interval data uncertainty where all realizations between pre-determined intervals are possible. Unlike the aforementioned studies, Keyvanshokooh et al. (2016) consider multi-period planning for a closed-loop supply chain design, incorporating strategic decisions related to the facility location and capacity and tactical decisions related to production planning and shipment. The authors define polyhedral uncertainty sets that include the budget of uncertainty within the interval model. However, these works treat the demand uncertainty as exogenous to the problems. We incorporate the idea of the dependency of demand realizations as proposed by Ardjmand et al. (2016) for the robust multi-period production planning problem into the proposed robust multi-period supply chain design problem, including production planning and product pricing decisions.

We conduct a case study on the Benelux region for the implementation of a CO_2-based syngas supply chain by applying the proposed robust multi-period supply chain design formulation to data generated based on expert elicitation, literature, and technical reports, where different scenarios and parameter settings are considered. As an expert elicitation method, we employed the Delphi method, consisting of multiple rounds of getting expert opinions on research questions until consensus is reached on answers (Withanaarachchi et al., 2015). We prepared two rounds of a questionnaire and organized a workshop in the third round. We gathered the opinions of experts from sectors, including the fossil fuel industry, CO_2 capture and purification industry, funding bodies, electrolysis technology developers, chemical industry, and academia, and asked their views on the price of grid electricity, capital costs of electrolyzers, government financial incentives, and regulatory support, among others. The detailed results of the data obtained from the Delphi method can be found at the link https://edu.nl/bpxfh.

The managerial and design insights derived from our case study fill the knowledge gaps of a CO_2-based syngas supply chain design by presenting quantitative results on the following aspects:

- Demand uncertainty: A robust design ensures feasibility in all demand scenarios and reduces syngas production costs significantly in worst-case conditions.

- Renewable electricity availability: In a centralized design for multiple countries, electrolysis plants are mainly located in the country with the lowest grid-related emissions. While this increases syngas transportation distances, it reduces overall costs by minimizing investments in renewable electricity generation, the largest cost component, resulting in lower syngas prices.
- Trade-off between battery and electrolyzer capacities: When battery costs and degradation rates are high, larger electrolyzers are preferable for maximizing renewable electricity use instead of relying on batteries. If electrolysis plants operate flexibly without fixed schedules, production becomes discontinuous. However, with fixed operating hours, batteries are heavily used for storage, allowing for smaller electrolyzer installations.
- Government financial support: Increased financial support for capital and operational expenses reduces costs both directly and indirectly because it provides more options for strategic infrastructure and location decisions. For example, higher financial support can enable the inclusion of large syngas demand sites that would otherwise be excluded due to high marginal costs, can lead to lower transportation investments by mitigating the impact of grid differences between countries on electrolysis plants locations, and can allow higher battery installations to increase renewable electricity usage.

The rest of the work is organized as follows. In Section 2, we explain the assumptions used to define the supply chain problem model. Later, the problem definition and mathematical models are provided, first defining the deterministic setting and then introducing demand uncertainty for the robust version. In Section 3, we present the results of computational experiments. We show the value of considering the demand uncertainty while designing the supply chain of CO_2-based syngas and investigate the effects of important factors, such as government financial supports, battery usage, and renewable electricity variability, on economic analyses of the supply chain under different parameter settings. In Section 4, we present concluding remarks and some future research directions.

2. Methodology

Modeling assumptions

To design a realistic supply chain that has time-dependent and uncertain parameters, we employ a multi-period planning approach to incorporate the changes in the parameters over time and include pricing decisions to consider economic feasibility while respecting the targeted carbon footprint level of the electricity consumed during production and employ a robust optimization approach to have a design that is immune to the demand uncertainty. The multi-period planning of supply chain design is also compatible with scaling up the CO_2E technology over time, where the use of technology is gradually expanded until widespread adoption, i.e., the set of syngas consumers to be served in each period is a decision and its size is nondecreasing over periods. In the case study, while modeling the supply chain design, we use the following assumptions:

- Solid oxide electrolyzers are used for CO_2 electrolysis. A stack lifetime is 5 years (Detz et al., 2023), after which the stack is replaced leading to replacement costs.
- Electricity usage is modeled based on bidding zones, which differ across the Netherlands, Belgium, and Luxembourg (European Network of Transmission System Operators for Electricity, 2021). Statistical data shows that grid characteristics, like the penetration of renewable sources and the global warming potential of non-renewable sources, can be different for these countries. Hence, we assume that grid characteristics depend on zones. Investments in renewable electricity are made based on zones. If renewable electricity generation plants are located in a zone, they can provide electricity to multiple electrolysis plants whose locations are in the same zone and other pre-determined zones.
- CO_2 and syngas are only transported by pipelines because pipeline transportation is the most common mode for CO_2 (Metz et al., 2005; Nguyen et al., 2023) and the primary mode for syngas (European Industrial Gases Association, 2022; Linde Gas, 2024). CO_2 pipelines connect CO_2 sources to electrolysis plants and syngas pipelines connect electrolysis plants to syngas consumers. Maximum allowable pipeline lengths are imposed for CO_2 and syngas. As suggested by Hasan et al. (2014), we set a maximum length for each CO_2 pipeline. For each syngas pipeline, a maximum length is also set due to safety concerns related to the flammability and toxicity of syngas (European Industrial Gases Association, 2022). No pipelines are assumed to exist at the beginning of the planning horizon.
- Batteries can be located on-site at electrolysis plants. We consider lithium-ion (Li-ion) batteries (Jung et al., 2020) because they have the greatest share in the total installed capacity (IEA, 2023) compared to other types of batteries in the industrial sector. Specifically, 4-hour Li-ion batteries are considered because they are mostly used in utility-scale battery storage (IEA, 2023). Battery capacity degradation, affected by factors such as varying cell temperature, charge and discharge amounts, and time spent for charging and discharging (Vermeer et al., 2021), is simplified by assuming a fixed degradation rate over periods.
- To reduce computational complexity related to the capacity-cost functions, the capacities of electrolyzers and batteries are defined as continuous variables. However, to account for the impact of economies of scale (Store & Go, 2019b), the electrolysis plants are categorized as small and large plants, with varying installation costs for electrolyzers per unit capacity. The overall capacity of electrolyzers in a large-scale electrolysis plant is from 50 to 1000 MW, whereas the total capacity of electrolyzers in a small-scale electrolysis plant is up to 50 MW. The 50 MW threshold is based on the information presented in the report of Store & Go (2019b) because the cost function for capacity installations has a breakpoint at 50 MW once the other breakpoints are set to capacities of 0 and 1000 MW. The function is approximated by a piecewise linear function, i.e., the cost of unit capacity installation between two breakpoints does not change.
- The planning horizon, with the start and end years of 2030 and 2050, has four 5-year periods. Each year consists of 365 days with 24 hours. The demands for syngas occur annually. To alleviate the computational burdens caused by a large number of decision variables and constraints, annual production decisions for satisfying annual demands are the same and repeated for every 5 years in a period (Wolff et al., 2023). The annual demands, share of renewable sources in the grid, and the grid electricity price remain the same during a period.
- Multi-period supply chain design problems involving capacitated facility location decisions can consider different capacity expansion strategies for facilities at different layers (Melo et al., 2009). We consider capacity expansions for electrolysis plants, batteries, and renewable electricity generation plants. To align with the increasing demand over time, as suggested by the Delphi method for our case study, we assume non-decreasing capacity expansions for these facilities (Melo et al., 2006). In each period, capacity expansions are allowed up to a predefined limit determined by the capacity expansion factor (Li et al., 2023b).
- For customer satisfaction, if a demand site is served in a period, its demand is fully satisfied. If a demand site is once served, it should remain served until the end of the planning horizon.

- The electricity consumption at electrolyzers is measured in kWh, aligning with how grid electricity prices are typically reported (Eurostat, 2024d), while the capacity of renewable electricity generation plants is usually specified in kW (European Commission, 2024c,b). Accordingly, investments in renewable sources are made in kW, or MW, and the total electricity generated from renewable sources is converted into kWh, or MWh to ensure consistency with grid electricity usage. To calculate the total electricity generated by renewable plants, we use capacity factors associated with renewable sources. The capacity factor is a pre-calculated ratio obtained by dividing the annual gross electricity generation by the net capacity, assuming 8760 operating hours per year (IEA, 2021a).

Problem definition

The problem focuses on optimizing a multi-period supply chain for CO_2-based syngas production using captured CO_2, water, and electricity, where the demand uncertainty is taken into account. The supply chain network includes CO_2 sources where CO_2 is captured, potential electrolysis plant sites where the syngas is produced if a plant is located, and syngas demand locations where the syngas is consumed. The electricity needs of electrolysis plants are satisfied by the electricity from the grid, renewable sources, and batteries if installed. With the pipeline infrastructure, CO_2 is transported from CO_2 sources to electrolysis plants, respecting the amount of CO_2 captured at sources and the capacities of the plants, and syngas is transported from electrolysis plants to demand sites, respecting the capacities of plants and demands of demand sites. There are estimations for the demand realized at each demand site, and the decisions are taken to have a supply chain that is robust to the uncertainty in demand. Strategic decisions made at the beginning include selecting plant locations, installing CO_2 capture systems, building pipelines, and setting initial capacities and syngas prices. These decisions are followed by tactical decisions in each time period, such as expanding capacities, planning production, sourcing electricity from the grid or renewables, and determining which customers to serve.

The problem considers economic and environmental concerns. In the environmental aspect, an emission limit is set for the electricity consumed during production. Renewable electricity generation and storage options are taken into account. For the economic aspect, overall revenue and cost in the system are considered. While the overall cost depends on all investments and planning, the overall revenue depends on the syngas price and price-sensitive demands. In light of these considerations, the aim is to maximize the net present value of the supply chain by balancing costs, revenues, and environmental impact over time.

Mathematical models

In this section, we first define the supply chain design problem in the deterministic setting and then incorporate the demand uncertainty into the problem via a robust formulation. Sets, decision variables, and parameters used in this section are provided in the Appendix in Table 5. Note that parameters are represented by symbols in this section to demonstrate the adaptability of the proposed formulations to various datasets. The specific numerical values assigned to these parameters based on our case study are provided in Section 3.1.

The supply chain network includes the set of CO_2 sources represented by C, the set of potential locations for electrolysis plants represented by E, the set of syngas demand sites represented by S. Set E may include CO_2 sources or syngas demand sites, i.e., $E \subseteq C \cup S \cup E'$ where $E' \cap (C \cup S) = \emptyset$. The set L represents the set of potential price levels for the CO_2-based syngas. The set R represents the set of zones where the renewable electricity generation plants are located. Renewable electricity transmission within zones can be allowed. Accordingly, o^e_{ij} represents if the renewable electricity transmission is allowed between zones $i, j \in R$; it is 1 if allowed and 0 otherwise. Additionally, o_{ij} represents the relation between electrolysis plant location $i \in E$ and zone $j \in R$; it is 1 if the location is in the zone and 0 otherwise. Note that $o^e_{jj} = 1$ for all $j \in R$ and $\sum_{j \in R} o_{ij} = 1$ for all $i \in E$. The set T represents the set of periods in the planning horizon. Time-dependent parameters and decision variables are given with index t, which represents the period $t \in T$.

There are two different types of flow in the supply chain: CO_2 flows are between CO_2 sources and electrolysis plants and syngas flows are between electrolysis plants and syngas demand sites. To transport these flows, pipelines are used. Installing pipelines for CO_2 and syngas per km costs f^c and f^s, respectively, where the distance between CO_2 source $i \in C$ and potential electrolysis plant location $j \in E$ is d^{ce}_{ij} and the distance between plant location $i \in E$ and demand site $j \in S$ is d^{es}_{ij}. At the CO_2 source $i \in C$, installing CO_2 capture technology costs f^{cap}_i, and at most g^c_i tonnes of CO_2 can be captured. After CO_2 is captured, it is transported to CO_2 electrolysis plants to be utilized, where the maximum length of a CO_2 pipeline between two endpoints is set to M^c. In the utilization process, CO_2 and water are electrolyzed and converted into syngas. Each electrolysis plant annually operates up to total hours of h. To produce one tonne of syngas at an electrolysis plant, a^c tonnes of CO_2, a^e MWh of electricity, and a^w tonnes of water are required. The price of one tonne of water consumed is p^w.

Electrolyzer investment costs differ for small and large-scale electrolysis plants due to the economies of scale. Installing one kW capacity of electrolyzer in period $t \in T$ results in capital cost (CAPEX) of $\kappa^{e,s}_t$ for small-scale electrolysis plants and of $\kappa^{e,l}_t$ for large-scale electrolysis plants. Fixed operational costs (OPEX) of electrolyzers occur annually where $\omega^{e,s}_t$ and $\omega^{e,l}_t$ represent the operational costs of small- and large-scale electrolysis plants in period $t \in T$, respectively.

Each electrolysis plant can use electricity from the grid and electricity from renewable sources. Additionally, if batteries are located with an electrolysis plant, surplus electricity from renewable sources can be stored in batteries to be later used by that plant. To use renewable electricity, investments in renewable energy plants are made. Investments in renewable electricity generation plants in period $t \in T$ result in CAPEX of κ^r_t and OPEX of ω^r_t. To store the renewable electricity, batteries should be installed. Batteries are installed on-site with electrolysis plants, where battery installation in period $t \in T$ has a CAPEX of κ^b_t and OPEX of ω^b_t. In each period, expansion of the capacity is allowed for electrolysis plants, renewable electricity generation plants, and batteries, but only up to a percentage of exC, depending on the capacity already installed in the previous period. The annual price for using one MWh of electricity from the grid in period $t \in T$ is p^e_t. There exists a maximum allowed global warming potential (GWP) allocated to the electricity consumed during syngas production, which is represented by u^{gwp}. To calculate the GWP of electricity from the grid in zone $i \in R$, the carbon footprints of electricity generated from renewable and non-renewable sources, represented by GWP^r_i and GWP^{non-r}_i, respectively, are used. Accordingly, the carbon footprint of the grid electricity in zone $i \in R$ in period $t \in T$ is calculated as $(1 - \eta_{it})GWP^{non-r}_i + \eta_{it} GWP^r_i$, where η_{it} is the share of renewables in the grid.

While grid electricity is always available, renewable electricity is intermittent and enabled by the investments made. The capacity factor, which converts power to electricity, of renewable sources in zone $i \in R$ in period $t \in T$ is represented by μ_{it}. Accordingly, MW of capacities for renewable electricity plants are converted to MWh of capacities for renewable electricity production by using the capacity factors. The variability of renewable electricity supply is given as the percentage of the total operating hours of electrolysis plants when direct renewable electricity, i.e., excluding electricity stored in batteries, cannot be used due to low supply. Note that the variability level in renewable electricity supply and capacity factor of renewable electricity generation plants are different because the variability level focuses

on how long renewable electricity is directly available for electrolysis plants, whereas the capacity factor measures how much electricity is actually generated compared to the maximum possible output. The percentage of variability in renewable electricity is represented by ν. Renewable electricity can be stored in batteries, if not directly used, up to the installed battery capacity at each electrolysis plant. Note that a percentage, presented by l^b, of battery capacities is lost in each period because of degradation.

After syngas is produced in electrolysis plants, it is transported to syngas consumers. Syngas pipelines have a maximum length of M^s. Each price level $l \in L$ corresponds to a price of syngas represented by pr_l. The minimum and maximum prices are represented by PL and PU, respectively. Each syngas consumer $i \in S$ has an annual demand of d_{itl} for the price level $l \in L$ in period $t \in T$. Note that if demands are deterministic, the annual demand at each customer site will be a pre-determined value. However, if demands are uncertain, they will be realized based on pre-defined distributions, scenarios, or uncertainty sets. In our work, we employ an uncertainty set for demand realizations.

The supply chain design decisions are taken over a multi-period planning horizon. At the beginning of the planning horizon, long-term decisions such as location, pipeline infrastructure, and initial capacity allocation decisions are made. The CO_2 capture facilities are located at CO_2 sources, and y_i^c denotes if a CO_2 capture technology is employed at CO_2 source $i \in C$, i.e., $y_i^c = 1$ if CO_2 is captured from that source; 0 otherwise. The electrolysis plants are located, where $y_i^{e,s}$ and $y_i^{e,l}$ denote whether a small-scale and a large-scale electrolysis plant is located at $i \in E$, respectively. The initial capacities of electrolysis plants are determined, and electrolyzers are installed at these plants. The initial capacities of small and large-scale electrolysis plants are represented by $n_i^{k,s}$ and $n_i^{k,l}$, respectively. Additionally, the batteries can be used at electrolysis plants, where n_i^b denotes the installed capacity in the electrolysis plant $i \in E$. Investments can be made in renewable sources, where n_i^r represents the initial capacity of renewable electricity generation plants – such as wind turbines or solar panels – installed in zone $i \in R$. The price of CO_2-based syngas is determined by choosing a price level from a set of potential price levels, and ρ_l indicates if the price level $l \in L$ is chosen or not, i.e., $\rho_l = 1$ if price level l is chosen; 0 otherwise. For the pipeline infrastructure, decisions regarding whether there is a pipeline between two sites are made, where θ_{ij}^c denote if there is a pipeline between CO_2 source $i \in C$ and electrolysis plant $j \in E$ and θ_{ij}^s denote if there is a pipeline between electrolysis plant $i \in E$ and syngas consumer $j \in S$.

At the beginning of each period, the medium-term decisions related to capacity expansions of electrolysis plants, batteries, and renewable electricity generation plants, customer allocations, delivery schedules, and production planning are made. Respectively, in period $t \in T$, while z_{it} represents if the syngas customer $i \in S$ is served or not, $n_{it}^{k,s}$ and $n_{it}^{k,l}$ and n_{it}^b denote the capacities of electrolyzers and batteries at electrolysis plant $i \in E$, and n_{it}^r denotes the total capacity of renewable electricity generation plants in zone $i \in R$. To satisfy the annual demands of customers, production planning and delivery decisions are repeated in a period. Accordingly, in each year of period $t \in T$, q_{it}^c tonnes of CO_2 are captured at the CO_2 source $i \in C$, x_{ijt}^c tonnes of CO_2 are transported via the pipeline between the CO_2 source $i \in C$ and the electrolysis plant $j \in E$, q_{it}^s tonnes of syngas are produced by using e_{it}^g MWh of electricity from the grid, e_{it}^r MWh of direct renewable electricity, and e_{it}^b MWh of stored renewable electricity in batteries at the electrolysis plant $i \in E$, and x_{ijt}^s tonnes of CO_2-based syngas are transported via the pipeline between electrolysis plant $i \in C$ and syngas consumer $j \in S$.

Fig. 3 shows when and which decisions are taken for the given planning horizon. The electricity usage decisions result in an environmental impact. Hence, we constrain the global warming potential of the electricity consumed during the production per tonne of syngas produced at each electrolysis plant $i \in E$ in each period $t \in T$ which is calculated as follows

$$\frac{GWP^r e_{it}^r + GWP_{jt}^g e_{it}^g}{a^e q_{it}^s},$$

where zone $j \in R$ is the zone in which the associated electrolysis plant is located, i.e., $o_{ij} = 1$. The decisions result in a monetary impact. To have a realistic investment plan for the supply chain design, we consider the net present value of these monetary flows taking into account the time value of money, where the interest rate is represented by I. Firstly, we define a function that represents the present value of total costs, including initial investments in small and large electrolysis plants, batteries, renewable electricity plants, CO_2 capture systems, and pipeline infrastructure for CO_2 and syngas; capacity expansion costs for small and large electrolysis plants, batteries, and renewable electricity plants; stack replacement costs for small and large electrolysis plants; annual fixed operational costs for small and large electrolysis plants and batteries, water and grid electricity usage costs to produce syngas at electrolysis plants, and annual fixed operational costs for renewable electricity plants. The value of function $PC(\mathbf{n^{e,s}}, \mathbf{n^{e,l}}, \mathbf{n^r}, \mathbf{n^b}, \mathbf{y^c}, \boldsymbol{\theta^c}, \boldsymbol{\theta^s}, \mathbf{q^s}, \mathbf{e^g})$ is calculated by summing the following terms

$$\sum_{i\in E}(\kappa_0^{e,s} n_{i0}^{e,s} + \kappa_0^{e,l} n_{i0}^{e,l} + \kappa_0^b n_{i0}^b) + \sum_{i\in R}\kappa_0^r n_{i0}^r + \sum_{i\in C} f_i^{cap} y_i^c + \sum_{i\in C}\sum_{j\in E} f^c d_{ij}^{ce}\theta_{ij}^c + \sum_{i\in E}\sum_{j\in S} d_{ij}^{es} f^s \theta_{ij}^s,$$

$$\sum_{t\in T}\left(\sum_{i\in E}\frac{\kappa_t^{e,s}(n_{it}^{e,s} - n_{i,t-1}^{e,s}) + \kappa_t^{e,l}(n_{it}^{e,l} - n_{i,t-1}^{e,l}) + \kappa_t^b(n_{it}^b - n_{i,t-1}^b)}{(1+I)^{5(t-1)}} + \sum_{i\in R}\frac{\kappa_t^r(n_{it}^r - n_{i,t-1}^r)}{(1+I)^{5(t-1)}}\right) + \sum_{t\in T:t\geq 2}\sum_{i\in E}\frac{\psi_t^s n_{i,t-1}^{e,s} + \psi_t^l n_{i,t-1}^{e,l}}{(1+I)^{5(t-1)}},$$

$$\sum_{t\in T}\sum_{t'=1}^{5}\left(\sum_{i\in E}\frac{\omega_t^{e,s} n_{it}^{e,s} + \omega_t^{e,l} n_{it}^{e,l} + \omega_t^b n_{it}^b + \left(a^w p_t^w q_{it}^s + p_t^e e_{it}^g\right)}{(1+I)^{5(t-1)+t'}} + \sum_{i\in R}\frac{\omega_t^r n_{it}^r}{(1+I)^{5(t-1)+t'}}\right).$$

Secondly, the present revenue is calculated based on the interest rate, the amount of demands served, and the price of syngas. We consider the dependency between the demand and price, where the demand decreases as the price increases. To alleviate the computational burdens, we discretized the function of this dependency instead of considering a continuous one as suggested by Ardjmand et al. (2016) and Fattahi et al. (2018). Hence, depending on the price level chosen, demands will change. We employ the following equation, which is proposed by Fattahi et al. (2018),

$$d_{itl} = d_{it}^{base} \times \left(\frac{PU - pr_l}{PU - PL}\right), \tag{2}$$

where d_{it}^{base} represents the base demand, i.e., the amount of demand when the price is minimum, for demand site $i \in S$ in period $t \in T$. Based on this equation, the relationship between demand and price can be depicted as in Fig. 4. Respectively, considering the demand sites served and the price level chosen, the present value of total revenue is calculated in the same manner as the present cost.

Deterministic formulation

We propose the following multi-period mathematical formulation for the problem in the deterministic setting, i.e., assuming full knowledge of the problem parameters.

$$\max \sum_{l\in L}\sum_{t\in T}\sum_{i\in S}\sum_{t'=1}^{5}\frac{\rho_l z_{it} pr_l d_{itl}}{(1+I)^{5(t-1)+t'}} - PC(\mathbf{n^{e,s}}, \mathbf{n^{e,l}}, \mathbf{n^r}, \mathbf{n^b}, \mathbf{y^c}, \boldsymbol{\theta^c}, \boldsymbol{\theta^s}, \mathbf{q^s}, \mathbf{e^g}) \tag{3.1}$$

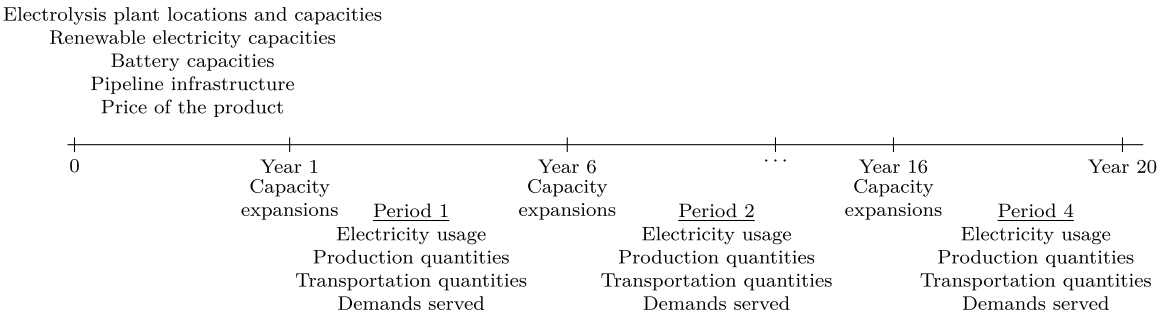

Fig. 3. Decisions taken over the planning horizon.

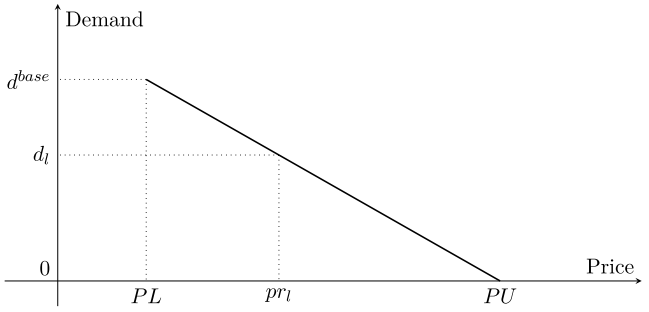

Fig. 4. Price-dependent demand function.

$$\text{s.t. } GWP^r e^r_{it} + GWP^g_{jt} e^g_{it} \le u^{gwp} a^e q^s_{it} \quad \forall i \in E, t \in T, j \in R : o_{ij} = 1 \tag{3.2}$$

$$z_{it} \le z_{i,t+1} \qquad \forall i \in S, t \in T \setminus \{|T|\} \tag{3.3}$$

$$y^{e,s}_i + y^{e,l}_i \le 1 \qquad \forall i \in E \tag{3.4}$$

$$y^{e,s}_i + y^{e,l}_i \le z_{i1} \qquad \forall i \in E \cap S \tag{3.5}$$

$$y^{e,s}_i + y^{e,l}_i \le y^c_i \qquad \forall i \in E \cap C \tag{3.6}$$

$$a^e q^s_{it} \le e^g_{it} + e^r_{it} \qquad \forall i \in E, t \in T \tag{3.7}$$

$$e^r_{it} - e^b_{it} \le h(1-\nu)\left(n^{e,s}_{it} + n^{e,l}_{it}\right) \qquad \forall i \in E, t \in T \tag{3.8}$$

$$e^b_{it} \le e^r_{it} \qquad \forall i \in E, t \in T \tag{3.9}$$

$$e^b_{it} \le 4 \times 365 \left(n^b_{i0}(1-l^b)^{t-1} + \sum_{t'=1}^{t} (n^b_{it'} - n^b_{i,t'-1})(1-l^b)^{t-t'} \right) \qquad \forall i \in E, t \in T \tag{3.10}$$

$$\sum_{j \in E} \left(o_{ji} e^r_{jt} + \sum_{k \in R \setminus \{i\}} o^e_{ik} o_{jk} e^r_{jt} \right) \le 24 \times 365 \left(\mu_{it} n^r_{it} + \sum_{k \in R \setminus \{i\}} o^e_{ik} \mu_{kt} n^r_{kt} \right) \qquad \forall i \in R, t \in T \tag{3.11}$$

$$q^c_{it} \le y^c_i g^c_i \qquad \forall i \in C, t \in T \tag{3.12}$$

$$\sum_{j \in E} x^c_{ijt} \le q^c_{it} \qquad \forall i \in C, t \in T \tag{3.13}$$

$$a^c q^s_{it} \le \sum_{j \in C} x^c_{jit} \qquad \forall i \in E, t \in T \tag{3.14}$$

$$\sum_{j \in S} x^s_{ijt} \le q^s_{it} \qquad \forall i \in E, t \in T \tag{3.15}$$

$$\sum_{l \in L} \rho_l z_{it} d_{itl} \le \sum_{j \in E} x^s_{jit} \qquad \forall i \in S, t \in T \tag{3.16}$$

$$\sum_{l \in L} \rho_l = 1 \tag{3.17}$$

$$L^j y^{e,j}_i \le n^{e,j}_{it} \le U^j y^{e,j}_i \qquad \forall i \in E, j \in \{s,l\}, t \in T \tag{3.18}$$

$$n^b_{i,|T|} \le M(y^{e,s}_i + y^{e,l}_i) \qquad \forall i \in E \tag{3.19}$$

$$q^s_{it} \le \frac{h\left(n^{e,s}_{it} + n^{e,l}_{it}\right)}{a^e_t} \qquad \forall i \in E, j \in \{s,l\}, t \in T \tag{3.20}$$

$$n^{e,j}_{i,t-1} \le n^{e,j}_{it} \qquad \forall i \in E, j \in \{s,l\}, t \in T \tag{3.21}$$

$$n^b_{i,t-1} \le n^b_{it} \qquad \forall i \in E, t \in T \tag{3.22}$$

$$n^r_{i,t-1} \le n^r_{it} \qquad \forall i \in R, t \in T \tag{3.23}$$

$$n^{e,j}_{it} \le (1 + exC) n^{e,j}_{i,t-1} \qquad \forall i \in E, j \in \{s,l\}, t \in T \tag{3.24}$$

$$n^b_{it} \le (1 + exC) n^b_{i,t-1} \qquad \forall i \in E, t \in T \tag{3.25}$$

$$n^r_{it} \le (1 + exC) n^r_{i,t-1} \qquad \forall i \in R, t \in T \tag{3.26}$$

$$\theta^c_{ij} = 0 \qquad \forall i \in C, j \in E : d^{ce}_{ij} > M^c \tag{3.27}$$

$$\theta^s_{ij} = 0 \qquad \forall i \in E, j \in S : d^{es}_{ij} > M^s \tag{3.28}$$

$$x^c_{ijt} \le M \theta^c_{ij} \qquad \forall i \in C, j \in E, t \in T \tag{3.29}$$

$$x^s_{ijt} \le M \theta^s_{ij} \qquad \forall i \in E, j \in S, t \in T \tag{3.30}$$

$$y^{e,j}_i \in \{0,1\} \qquad \forall i \in E, j \in \{s,l\} \tag{3.31}$$

$$y^c_i \in \{0,1\} \qquad \forall i \in C \tag{3.32}$$

$$z_{it} \in \{0,1\} \qquad \forall i \in E, t \in T \tag{3.33}$$

$$\rho_l \in \{0,1\} \qquad \forall l \in L \tag{3.34}$$

$$n^{e,j}_i \ge 0 \qquad \forall i \in E, j \in \{s,l\} \tag{3.35}$$

$$n^b_i \ge 0 \qquad \forall i \in E \tag{3.36}$$

$$n^r_i \ge 0 \qquad \forall i \in R \tag{3.37}$$

$$\theta^c_{ij} \in \{0,1\} \qquad \forall i \in C, j \in E \tag{3.38}$$

$$\theta^s_{ij} \in \{0,1\} \qquad \forall i \in E, j \in S \tag{3.39}$$

$$e^g_{it}, e^r_{it}, e^b_{it} \ge 0 \qquad \forall i \in E, t \in T \tag{3.40}$$

$$q^c_{it} \ge 0 \qquad \forall i \in C, t \in T \tag{3.41}$$

$$q^s_{it} \ge 0 \qquad \forall i \in E, t \in T \tag{3.42}$$

$$x^c_{ijt} \ge 0 \qquad \forall i \in C, j \in E, t \in T \tag{3.43}$$

$$x^s_{ijt} \ge 0 \qquad \forall i \in E, j \in S, t \in T \tag{3.44}$$

The objective function (3.1) maximizes the present value of the profit over the planning horizon. Constraint (3.2) guarantees the maximum unit carbon footprint of electricity consumed at each electrolysis plant. Constraint (3.3) states that if a demand site is started to be served, then it needs to be served until the end of the planning horizon. Constraint (3.4) states that if an electrolysis plant is installed, it should be small-scale or large-scale. Constraints (3.5) and (3.6) guarantee that a customer site is served and that the carbon at a source is captured if an electrolysis plant is co-located with that demand site and CO_2 source, respectively.

Constraint (3.7) states that the total electricity required for syngas production is supplied, allowing for the use of both renewable and grid electricity. Constraint (3.8) considers the variability in renewable

electricity supply and allows the storage of renewable electricity in batteries in case of excess supply. In other words, since renewable electricity is not always available, a portion of it can be used directly for syngas production when available, while the excess can be stored in batteries for later use. Constraint (3.9) ensures that the electricity stored in batteries is not larger than the renewable electricity consumed in total at an electrolysis plant. Constraint (3.10) ensures that the electricity stored in batteries cannot be larger than the total operational capacity of batteries at the electrolysis plant, considering initial capacity and capacity expansions and degradation over periods. Constraint (3.11) limits the total renewable electricity consumed at electrolysis plants, considering the total renewable electricity generation capacity and renewable electricity transmission between zones. Note that the total capacity of renewable energy generation plants is converted into the total renewable electricity production considering the capacity factor and total operating hours of the renewable energy generation plants in a year.

Constraints (3.12)–(3.16) control the flow of CO_2 and syngas within the supply chain, ensuring that captured and transported amounts are regulated. Specifically, CO_2 can only be captured if a capture technology is employed, and its captured amount cannot exceed the available supply at the source. The amount of CO_2 transported to electrolysis plants is constrained by the amount captured at each source. Similarly, syngas production is dependent on the transported CO_2, and its distribution to demand sites cannot exceed production levels at electrolysis plants. Finally, if a syngas demand site is served, the delivery amount must be sufficient to meet its demand. Constraint (3.17) guarantees that only one price setting is selected to set the price of syngas. Constraint (3.18) sets lower and upper bounds on the capacities of electrolysis plants with respect to the scales of the electrolysis plants. Constraint (3.19) states that battery capacity installations are made for electrolysis plants. Constraint (3.20) restricts the amount of syngas produced by the total production capacity of the electrolysis plant, which is calculated based on its capacity (MW), total annual operating hours (h), and the amount of electricity needed to produce one tonne of syngas (MWh/tonne).

Constraints (3.21)–(3.26) state that capacity expansions are allowed for electrolysis plants, batteries, and renewable electricity sources, but only to a certain extent that is determined by the percentage capacity expansion factor. Constraints (3.27) and (3.28) ensure that if the distance between two sites is larger than the pre-determined distance, then there is no pipeline between these sites for CO_2 and syngas transportation, respectively. Constraints (3.29) and (3.30) state that no CO_2 and syngas flows can be sent, respectively, if there is no pipeline between two sites. Note that, for these constraints, values of Big M's can be updated as $\sum_{k\in C} g_k^c$ and $\sum_{k\in C} g_k^c/a^c$, respectively. Constraints (3.31)–(3.44) are domain constraints.

Note that Formulation (3) is not linear because there are bilinear terms in the objective function (3.1) and Constraint (3.16). We define a new decision variable ζ_{itl} that represents $\rho_l z_{it}$ for all $i \in S$, $t \in T$, and $l \in L$ and linearize it by using inequalities proposed by McCormick (1976). Hence, for the deterministic problem, the mixed integer linear programming formulation (MILP), which has a linear objective function and linear constraints along with some integer variables, can be given as follows:

Deterministic model

$$\max \sum_{l\in L}\sum_{t\in T}\sum_{i\in S}\sum_{t'=1}^{5} \frac{\zeta_{itl} pr_l d_{itl}}{(1+I)^{5(t-1)+t'}} - PC(\mathbf{n}^{e,s}, \mathbf{n}^{e,l}, \mathbf{n}^{r}, \mathbf{n}^{b}, \mathbf{y}^{c}, \theta^{c}, \theta^{s}, \mathbf{q}^{s}, \mathbf{e}^{g}) \tag{4.1}$$

s.t. (3.2)–(3.15), (3.17)–(3.44)

$$\sum_{l\in L} \zeta_{itl} d_{itl} \le \sum_{j\in E} x^s_{jit} \qquad \forall i \in S, t \in T \tag{4.2}$$

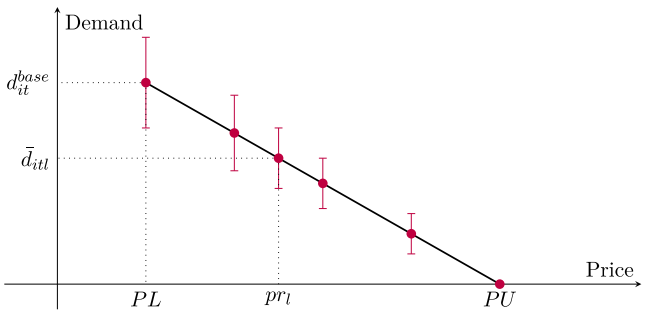

Fig. 5. Uncertainty sets for different price settings for the demand of syngas.

$$\zeta_{itl} \le z_{it} \qquad \forall l \in L, i \in S, t \in T \tag{4.3}$$

$$\zeta_{itl} \le \rho_l \qquad \forall l \in L, i \in S, t \in T \tag{4.4}$$

$$z_{it} + \rho_l - 1 \le \zeta_{itl} \qquad \forall l \in L, i \in S, t \in T \tag{4.5}$$

$$\zeta_{itl} \in \{0,1\} \qquad \forall i \in E, l \in L, t \in T \tag{4.6}$$

where Constraints (4.3) and (4.4) set $\boldsymbol{\zeta}$ to 0 when $\mathbf{z}$ or $\boldsymbol{\rho}$ are 0, and Constraint (4.5) sets $\boldsymbol{\zeta}$ to 1 when $\mathbf{z}$ and $\boldsymbol{\rho}$ are 1.

Robust formulation

In this section, we extend the deterministic formulation (4) to a robust formulation to account for demand uncertainty. In a general framework, uncertainty can arise in the coefficients of the objective function, the coefficients of constraints, or the right-hand sides of the constraints. The robust counterpart can be formulated based on different criteria, such as worst-case, best-case, or maximum regret, which measures the relative difference between two scenario performances (Gabrel and Murat, 2010). Each criterion has its implications. While the best-case criterion may result in infeasible solutions in most realizations, minimizing the maximum regret criterion can lead to intractable formulations (Gabrel and Murat, 2010). However, the worst-case criterion can guarantee the feasibility in all realizations while ensuring the computational tractability. In our work, we focus on demand uncertainty, where uncertainty affects both the objective function and constraint coefficients, and we adopt the worst-case criterion. To represent the demand uncertainty, we employ intervals, where the uncertain parameter is represented by an interval with a center called the nominal value (Soyster, 1973; Chinneck and Ramadan, 2000). We define the demand uncertainty set (5) that includes the demand realization intervals, i.e., demand realizations deviate from the nominal demand $\bar{d}_{itl}$ with respect to the robustness parameter γ_{it} for each $i \in S$ and $t \in T$ under price setting $l \in L$. When the demand uncertainty is incorporated into price-dependent demand, based on the idea proposed in Ardjmand et al. (2016), we can define the demand uncertainty set as follows:

$$\mathcal{D} = \Big\{ d \in \mathbb{R}_+^{|S|\times|T|\times|L|} : d_{itl} \in [\bar{d}_{itl}(1-\gamma_{it}), \bar{d}_{it}(1+\gamma_{it})] \quad \forall i \in S, t \in T, l \in L \Big\}. \tag{5}$$

For the better understanding of set (5), Fig. 5 depicts the demand realizations for varying price levels chosen. For syngas demand site $i \in S$ and period $t \in T$, the dot in red represents the nominal demand, and demands are realized between the range in red for the corresponding price level.

When the proposed uncertainty set is incorporated into the deterministic model, its robust counterpart can be given as follows:

$$\max \min_{d\in\mathcal{D}} \sum_{l\in L}\sum_{t\in T}\sum_{i\in S}\sum_{t'=1}^{5} \frac{\zeta_{itl} pr_l d_{itl}}{(1+I)^{5(t-1)+t'}} - PC(\mathbf{n}^{e,s}, \mathbf{n}^{e,l}, \mathbf{n}^{r}, \mathbf{n}^{b}, \mathbf{y}^{c}, \theta^{c}, \theta^{s}, \mathbf{q}^{s}, \mathbf{e}^{g}) \tag{6.1}$$

s.t. (3.2)–(3.15), (3.17)–(3.44), (4.3)–(4.6)

$$\max_{d\in D} \zeta_{itl} d_{it} \le \sum_{j\in E} x^s_{jit} \qquad \forall i \in S, t \in T. \tag{6.2}$$

The max–min objective function and maximization in the constraints can be straightforwardly linearized due to the advantages of the pure interval model (Solyalı et al., 2016), which preserves linearity and ensures boundedness in inner problems. As a result, the robust problem can be formulated as a mixed-integer linear programming model, given as follows:

Robust model

$$\max \sum_{l\in L}\sum_{t\in T}\sum_{i\in S}\sum_{t'=1}^{5} \frac{\zeta_{itl} pr_l \bar{d}_{itl}(1-\gamma_{it})}{(1+I)^{5(t-1)+t'}} - PC(\mathbf{n}^{\mathbf{e,s}}, \mathbf{n}^{\mathbf{e,l}}, \mathbf{n}^{\mathbf{r}}, \mathbf{n}^{\mathbf{b}}, \mathbf{y}^{\mathbf{c}}, \boldsymbol{\theta}^{\mathbf{c}}, \boldsymbol{\theta}^{\mathbf{s}}, \mathbf{q}^{\mathbf{s}}, \mathbf{e}^{\mathbf{g}}) \tag{7.1}$$

s.t. (3.2)–(3.15), (3.17)–(3.44), (4.3)–(4.6)

$$\zeta_{itl}\bar{d}_{itl}(1+\gamma_{it}) \le \sum_{j\in E} x^s_{jit} \qquad \forall i \in S, t \in T \tag{7.2}$$

where objective function (7.1) maximizes the present value of profit in the worst case, and Constraint (7.2) guarantees that the supply chain design is able to deal with all demand realizations.

3. Computational experiments on the case study data

In this section, we present and discuss the results we obtained after solving the proposed robust mathematical formulation for the case study data under different scenarios and parameter settings. With the computational results, we first show the value of considering demand uncertainty in the decision-making process of the supply chain design of CO_2-based syngas and then make economic analyses of the robust supply chain design under different government financial supports, operating hours for electrolysis plants, and levels of variability in renewable electricity supply.

We define a new indicator, the levelized cost of syngas (LCOS), for fair comparison of the results obtained under different settings because comparing objective function values such as total profits, may be misleading when the chosen price level and, accordingly, demands are different. The levelized cost of a product represents the break-even price for the product, i.e., it is the lowest price that should be set to obtain a nonnegative profit. Note that arrays are written in bold font, whereas their elements are written in regular font; this also applies to the numbers, e.g., **0** represents the array of 0's. We define the LCOS under the lowest demand realizations at each demand site. Let $\boldsymbol{\alpha}^* = (\mathbf{y}^{\mathbf{e,s}*}, \mathbf{y}^{\mathbf{e,l}*}, \mathbf{y}^{\mathbf{c}*}, \mathbf{z}^*, \rho^*, \boldsymbol{\zeta}^*, \boldsymbol{\theta}^{\mathbf{c}*}, \boldsymbol{\theta}^{\mathbf{s}*}, \mathbf{n}^{\mathbf{e,s}*}, \mathbf{n}^{\mathbf{e,l}*}, \mathbf{n}^{\mathbf{r}*}, \mathbf{n}^{\mathbf{b}*}, \mathbf{q}^{\mathbf{c}*}, \mathbf{q}^{\mathbf{s}*}, \mathbf{e}^{\mathbf{g}*}, \mathbf{e}^{\mathbf{r}*}, \mathbf{e}^{\mathbf{b}*}, \mathbf{x}^{\mathbf{c}*}, \mathbf{x}^{\mathbf{s}*})$ be the optimal solution to Formulation (7), then LCOS under the optimal solution of α^* can be given as follows:

$$LCOS(\boldsymbol{\alpha}^*) = \frac{PC(\mathbf{n}^{\mathbf{e,s}*}, \mathbf{n}^{\mathbf{e,l}*}, \mathbf{n}^{\mathbf{r}*}, \mathbf{n}^{\mathbf{b}*}, \mathbf{y}^{\mathbf{c}*}, \boldsymbol{\theta}^{\mathbf{c}*}, \boldsymbol{\theta}^{\mathbf{s}*}, \mathbf{q}^{\mathbf{s}*}, \mathbf{e}^{\mathbf{g}*})}{\sum_{t\in T}\sum_{t'=1}^{5}\sum_{i\in S}\sum_{l\in L} \frac{\zeta^*_{itl}\bar{d}_{itl}(1-\gamma_{it})}{(1+I)^{5(t-1)+t'}}}.$$

The computational experiments are performed on a 64-bit machine with 11th Gen Intel Core i7-11800H 2.30 GHz and 16 GB of RAM. The formulations are coded in Python using Gurobi 10.0.2. All instances are solved to optimality within an hour.

3.1. Details of the case study data instances

In this section, we explain the data used in the computational experiments. Note that the data files used for solving the models and the robust model code can be found at https://edu.nl/bpxfh.

In the computational experiments, the Benelux network, generated by Wiltink et al. (2023), is used. The network includes the locations of CO_2 sources, current syngas users (e.g., industrial clusters), potential electrolysis plant locations, and the arcs between each CO_2 source and potential electrolysis plant location pair and each potential electrolysis plant location and current syngas user pair. The lengths of the arcs represent the geographic distances between sites (Wiltink et al., 2023). Fig. 6 depicts the locations of CO_2 sources by dots, syngas consumers by triangles, and potential electrolysis plants by diamonds. There are 49 CO_2 sources, 10 syngas demand sites, some of which overlap in the figure because they are closely located to each other, and 83 potential electrolysis plant locations. Potential electrolysis plant locations include the locations of CO_2 sources and syngas consumers and intermediate locations between certain CO_2 sources and syngas consumers if sufficient space is available. For CO_2 sources, only biogenic sources, which are biomethane fermentation, bioethanol fermentation, pulp and paper, and non-hazardous waste incineration plants, are considered. Only biogenic CO_2 sources are considered to align with the statement by European Commission (2024a), ensuring that carbon management technologies are still effective in carbon mitigation after carbon neutrality in 2050. Since there is no carbon price for emissions from biogenic sources provided by the EU emissions trading systems (ETS), we disregard carbon pricing in the decision-making process. For CO_2 amounts at CO_2 sources, $\mathbf{g}^{\mathbf{c}}$, the data used in Wiltink et al. (2023) is used, and for the cost of employing CO_2 capture technologies at different types of CO_2 sources is calculated by employing piecewise linear approximation functions generated by Wiltink et al. (2023) with the assumption of that at least 75% of total carbon are captured at a source when a capture technology is installed. For the sets of zones for electricity consumption, R is set to $\{1, 2, 3\}$, where zone 1 represents the Netherlands, zone 2 represents Belgium, and zone 3 represents Luxembourg. The size of the set of price levels, $|L|$, is set to 50.

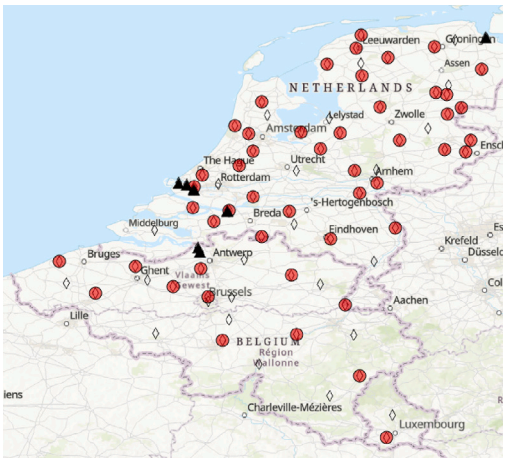

Fig. 6. Benelux map generated on ArcGIS Pro 3.4.0.

We consider that the planning horizon length is 20 years with 4 periods, i.e., $T = \{1, 2, 3, 4\}$. The first period starts in the year 2030, and the last period ends in the year 2050, which is compatible with the climate goals for 2050. Since some parameters are expected to change over time, they are defined as time-dependent. These are cost-related parameters such as $\kappa^{e,s}_t$, $\kappa^{e,l}_t$, ψ^s_t, ψ^l_t, κ^b_t, κ^r_t, $\omega^{e,s}_t$, $\omega^{e,l}_t$, ω^b_t, ω^r_t, and p^e_t, and technical parameters such as $\eta_{.t}$, $\mu_{.t}$, and GWP^g_t. The values of these parameters are assigned based on the literature and expert opinions obtained via the Delphi method. According to the results we obtained, with respect to the reference period of period 1, nominal demands will increase by 25% in the second period, 35% in the third period, and 40% in the fourth period. Grid electricity prices will increase by 20% in the second period, 10% in the third period, and remain the same in the fourth period. The share of renewables in the grid will increase by 15%, 35%, and 55% in the second, third, and fourth periods, respectively. Furthermore, with respect to the reference period of period 0, the

CAPEX of electrolyzers is expected to remain the same in the first two periods, decrease by 15% in the third period, and decrease by 25% in the fourth period.

The CAPEX of electrolyzers in the period 0 is 2000 EUR_{2019}/MW (Institute for Sustainable Process Technology (ISPT), 2023) for large-scale electrolysis plants. The economies of scale function is derived based on Store & Go (2019a), and it is assumed that a small electrolysis plant has a capacity less than 50 MW with CAPEX of 2500 EUR_{2019}/kW. For each $i \in \{s,l\}$ and $t \in T \cup \{0\}$, $\omega_t^{e,i}$ is calculated as 4% of $\kappa_t^{e,i}$ (Galkin et al., 2023) and ψ_t^i is calculated as 14% of $\kappa_t^{e,i}$ (Detz et al., 2023). The nominal demands in period 1 are considered as the expected amount of syngas currently consumed by demand sites (Wiltink et al., 2023). The grid electricity price in period 1 for all zones is 53.65 EUR_{2019}/MWh, which is the price for consumption over 150,000 MWh excluding taxes and levies (Eurostat, 2024c). The share of renewables in the grid in period 1 for all zones, if not otherwise stated, is considered as the share of renewable sources in electricity generation for Europe, which is 41% calculated based on the data on Eurostat (2023a,b).

The changes in CAPEX of renewable electricity generation plants and batteries are considered based on the literature. Accordingly, with respect to the reference period of period 0 over periods, the CAPEX of on-shore wind turbines will decrease by 8%, 11%, 14%, and 18% (Clean Energy Technology Observatory, 2023) and the CAPEX of Li-ion batteries will decrease by 25%, 35%, 45%, and 55% (Clean Energy Technology Observatory, 2024). Note that, for the renewable electricity generation plants, on-shore wind turbines are considered because, in the preliminary computational experiments, we observed that on-shore wind turbines are always selected for investments when we provide several options, including on-shore wind turbines, off-shore wind turbines, and solar panels, for renewable electricity investments. The optimal solutions do not suggest investments in off-shore wind turbines because of high investment costs and solar panels because of low capacity factors for Benelux countries, where CAPEX of off-shore wind and solar electricity are 1820 and 623 EUR_{2019}/kW and OPEX of them are 2.5% and 1.1% of CAPEX, respectively, Sens et al. (2022), and capacity factors of off-shore wind and solar electricity are 0.27 and 0.10, respectively (Eurostat, 2024a,b; Statista, 2024b). CAPEX of on-shore wind electricity and Li-ion batteries in period 0 is 1315 and 1700 EUR_{2019}/kW, respectively, while for each $t \in T \cup \{0\}$, ω_t^r is 1.1% of κ_t^r, and ω_t^b is 2.5% of κ_0^b (Sens et al., 2022; National Renewable Energy Laboratory, 2023). The battery percentage capacity loss is considered as 30% (Vermeer et al., 2021). The capacity factor of on-shore wind electricity for each period $t \in T$ is 0.24, which is derived based on the data provided (Eurostat, 2024a,b), and since there are no significant differences in capacity factors over years for the countries considered, the capacity factor of the renewable electricity is considered the same over the planning horizon.

In electrolysis plants, electrolyzers convert CO_2 and H_2O into syngas. There can be different ratios of H_2:CO by high temperature electrolysis (Dittrich et al., 2019). In computational experiments, we consider the production of syngas with a 2:1 hydrogen to carbon monoxide ratio. Accordingly, as reported in IEA Greenhouse Gas (2023), to produce 1 tonne of syngas, 1.36 tonne of CO_2, 1.16 tonne of H_2O, and 8.91 MWh of electricity are required with an electrolyzer efficiency of 100%. However, due to technological reasons, it may be difficult to obtain the conversion rate of 100%, and thus we consider 85% conversion efficiency (Institute for Sustainable Process Technology, 2023). In this regard, a^c is 1.60, a^w is 1.37, and a^e is 10.48.

We consider electricity generated from solar, on-shore wind, and offshore wind sources as renewable with an average carbon footprint of 20 kg CO_2-eq/kWh and electricity generated from coal and natural gas sources as non-renewable sources with an average carbon footprint of 715 kg CO_2-eq/kWh (Nowtricity, 2021). Hence, GWP_i^r and GWP_i^{non-r} are 20 kg CO_2-eq/kWh and 715 kg CO_2-eq/kWh for all $i \in R$, respectively, if not otherwise stated. We focus specifically on the carbon footprints associated with electricity consumption during the syngas production process, as efficient renewable energy integration is the most critical environmental factor for implementing CO_2E (Tsagkari et al., 2024). To calculate u^{gwp}, we consider that at least 90% of renewable electricity should be used in producing syngas, which is similar to the production of green hydrogen, i.e., if the share of renewables in the grid is 90%, the electrolyzers can be fully connected to the grid (European Parliment, 2023b). Accordingly, u^{gwp} is calculated as 89.5 CO_2-eq/kWh, i.e., $0.9 \times 20 + 0.1 \times 715$.

The costs of on-shore CO_2 and syngas pipelines, f^c and f^s, are 900 $kEUR_{2019}$ and 1000 $kEUR_{2019}$ per km, respectively (Van der Zwaan et al., 2011). Since there is not enough information on the cost of the syngas pipeline in the literature, we consider the cost of the hydrogen pipeline. The maximum distances for CO_2 and syngas pipelines, M^c and M^s, are 400 and 200 km, respectively. The maximum operating hours of electrolysis plants, h, is 8000. In each period, percentage capacity expansion factor, exC, of 50% is used for electrolyzers, renewable sources, and batteries. This factor is determined to ensure that capacity expansions align with demand growth, and thus is set to a value higher than the largest percentage increase in nominal demands over the planning horizon. For the water price, the price of process water of 0.36 EUR_{2019}/tonne is used (Intratec, 2024). An interest rate of 10% is considered to take into account the time value of the money (Timmerhaus and West, 2004).

In the computational experiments, we analyze the optimal solutions in terms of selected price, obtained profit, and calculated LCOS under different parameter settings. The parameter settings differ in the choices of price ranges ($PL-PU$), scenarios for grid characteristics and renewable electricity transmission and syngas and CO_2 transportation rules, robustness parameter (γ), levels of government financial support for electrolyzers, renewable electricity sources, and batteries, and the levels of variability in renewable electricity supply (ν). Three price ranges of PL-PU are selected as follows: 150–1500, 500–1850, and 150–3000. If not otherwise stated the price range of 150–3000 is used. Three different scenarios are considered for characteristics of grids and rules of renewable electricity transmission and syngas and CO_2 transportation.

- In Scenario 1, a common grid is used by all the electrolysis plants, where the share of renewables is chosen as the current average of European countries, renewable electricity transmission may be allowed between neighboring countries based on the regulation (European Commission, 2019), and the transportation of syngas and CO_2 is allowed between countries.
- In Scenario 2, unlike Scenario 1, we consider different grids for electrolysis plants that are located in different countries, where the share of renewables in the grid is calculated based on the statistical data of each country because the share of renewables and carbon footprint of non-renewables in the grid may be significantly different. In 2023, the grid of Belgium has a carbon footprint of 107 kg CO_2-eq/kWh and the share of renewables of 34%, and the grid of the Netherlands has a carbon footprint of 421 kg CO_2-eq/kWh and the share of renewables of 23% (Nowtricity, 2024a,b). Based on this data, it can be found that the average carbon footprint of non-renewable sources in Belgium is 151.82 and in the Netherlands is 540.77. This difference arises from the choices for sources of electricity, e.g., when there is not enough supply from sources like solar and wind, while Belgium prefers using electricity generated from nuclear energy, the Netherlands prefers generating electricity from coal and mainly natural gas. Since Luxembourg imports most of its electricity from abroad (Statista, 2024a) in 2023, the share of renewables and their carbon footprints are taken as the same as Belgium.

- Scenario 3 represents a decentralized planning where the planning is separately made for each country, where individual grids are used as in Scenario 2, and renewable electricity transmission and the syngas and CO_2 transportation between countries are not allowed.

The robustness parameter $\boldsymbol{\gamma}$ is chosen from the set of $\{\mathbf{0.1}, \mathbf{0.15}, \mathbf{0.2}, \mathbf{0.25}, \mathbf{0.3}, \boldsymbol{\gamma}^{\mathbf{T}}, \boldsymbol{\gamma}^{\mathbf{S}}\}$ to adjust the uncertainty level, where γ^T represents that the uncertainty decreases over time based on the assumption of the adoption of the technology increases over time, which an inference according to the Delphi method conducted, i.e., $\gamma_{i1} = 0.25, \gamma_{i2} = 0.2, \gamma_{i3} = 0.15$ and $\gamma_{i4} = 0.1$ for all $i \in E$, and γ^S represents that the uncertainty is less for the demand sites in the Netherlands than Belgium because of higher government regulatory supports based on the fact that the Netherlands currently has supporting policies for CO_2 capture and CCS projects while Belgium does not have a policy specifically for CCU or CCS projects (IEA, 2021b), i.e., for $t \in T$, $\gamma_{.t} = 0.1$ for syngas demand sites in the Netherlands and $\gamma_{.t} = 0.2$ for syngas demand sites in Belgium. In the computational experiments, different government financial supports for CAPEX of electrolyzers, renewable electricity sources, and batteries are considered because these costs constitute large shares of the LCOS, and thus they will play important roles in the financial aspects of syngas. Note that financial support can be provided through various mechanisms; however, in this study, we employ it as a percentage subsidy on CAPEX and thus OPEX. This approach facilitates a clear comparison between cases with differing levels of support and enables meaningful insights without requiring highly precise forecasts of future financial support policies. Let gfs represent the level of the financial support of governments to CAPEX, where the associated values are updated by being multiplied by $(1 - gfs)$. Unless otherwise stated, gfs is set to 0.5. In addition to financial support applied to CAPEX of electrolyzers, renewable electricity generation, and batteries, additional financial support may be employed for the CAPEX of batteries. Let $gfsB$ represent this additional financial support. Unless otherwise stated, $gfsB$ is 0. Lastly, we consider different levels of renewable electricity supply variability, ν chosen from the set $\{0.3, 0.4, 0.5, 0.6, 0.7\}$. It is chosen as 0.5 if not otherwise stated.

In the following sections, the results obtained from the computational experiments are summarized and analyzed. For the detailed results, we refer the reader to https://edu.nl/bpxfh.

3.2. The value of considering uncertainty

In this section, 47 instances that differ in price ranges, robustness parameter, and scenarios depending on features of the grid, renewable electricity transmission, and syngas and CO_2 infrastructure are solved to optimality for Formulations (4) and (7). The obtained results are compared to assess the value of considering uncertainty. Respectively, the performance of the optimal robust solution is compared with the optimal deterministic solution in the uncertain environment. The LCOS is used as a performance measure. For the given instance, first, the robust formulation (7) is solved, and the robust optimal solution $\boldsymbol{\alpha}^{\mathbf{r}}$ is obtained. Later, the deterministic formulation (4) is solved, and the deterministic optimal solution $\bar{\boldsymbol{\alpha}}^{\mathbf{d}}$ is obtained. When the uncertainty is not considered, strategic decisions will be made based on the deterministic solution because these decisions are made before the realization of the uncertainty, unlike tactical decisions. After the uncertainty is revealed, the deterministic decisions may even be infeasible because the initial capacities and infrastructure design cannot be respected. Hence, while considering the performances of solutions, we also allow repairs in the deterministic solution. These repairs include opening new small-scale electrolysis plants, increasing the initial capacity of renewable sources, and installing new pipeline connections for syngas or CO_2. Since these repair actions will be taken after the uncertainty is realized, they should be in operation within a short notice. Thus, only opening small-scale electrolysis plants is allowed, and employing extra capacities for renewable electricity generation and installing new pipeline connections costs 50% higher.

To evaluate the performance of solution $\bar{\boldsymbol{\alpha}}^{\mathbf{d}}$, Formulation (8) is solved to obtain the optimal solution $\boldsymbol{\alpha}^{\mathbf{detRe}}$ which represents the performance of the deterministic solution in the uncertain environment with repairs to avoid the infeasibility. $LCOS(\alpha^r)$ and $LCOS(\alpha^{detRe})$ are compared, and, for an instance, the value of considering uncertainty is calculated as $100\times\frac{LCOS(\alpha^{detRe})-LCOS(\alpha^r)}{LCOS(\alpha^r)}$. In all 47 instances, we observe that deterministic and robust strategic solutions differ, highlighting the impact of uncertainty on decision-making. To mitigate the risks associated with lower customer satisfaction and higher costs, the robust solutions result in different designs depending on the level of uncertainty. For example, at lower uncertainty levels, the robust designs usually propose higher initial capacities and alternative pipeline routes; at higher uncertainty levels, they usually propose the employment of different numbers of electrolysis plants to serve different sets of customers. Hence, considering uncertainty leads to higher profits by enabling more effective investment strategies that can deal with possible demand fluctuations. Even 21 instances end up with negative profits when the deterministic solution is used in the uncertain environment, i.e., the planning is first made according to the deterministic solution and repairs are made after uncertain demands are realized. In 43 out of 47 instances, there are decreases in the LCOS, which highlights the importance of employing the robust solution, in other words, the value of considering uncertainty in the decision-making process.

$$\max \sum_{l\in L}\sum_{t\in T}\sum_{i\in S}\sum_{t'=1}^{5}\frac{\zeta_{itl}\,pr_l\,\bar{d}_{itl}(1-\gamma_{it})}{(1+I)^{5(t-1)+t'}} - PC(\mathbf{n^{e,s}}, \mathbf{n^{e,l}}, \mathbf{n^{r}}, \mathbf{n^{b}}, \mathbf{y^{c}}, \boldsymbol{\theta}^{\mathbf{c}}, \boldsymbol{\theta}^{\mathbf{s}}, \mathbf{q^{s}}, \mathbf{e^{g}}) \tag{8.1}$$

$$-0.5\left(\sum_{i\in R}\kappa_0^r(n_{i0}^r-\bar{n}_{i0}^{r^d})+f^c d_{ij}^{ce}(\theta_{ij}^c-\bar{\theta}_{ij}^{c^d})+\sum_{i\in E}\sum_{j\in S}d_{ij}^{es}f^s(\theta_{ij}^s-\bar{\theta}_{ij}^{s^d})\right)$$

s.t. (3.2)–(3.15), (3.17)–(3.44), (4.3)–(4.6), (7.2)

$$\rho_l = \bar{\rho}_l^d \qquad \forall l \in L \tag{8.2}$$

$$y_i^c = \bar{y}_i^{c^d} \qquad \forall i \in C \tag{8.3}$$

$$\theta_{ij}^c \geq \bar{\theta}_{ij}^{c^d} \qquad \forall i \in C, j \in E \tag{8.4}$$

$$\theta_{ij}^s \geq \bar{\theta}_{ij}^{s^d} \qquad \forall i \in E, j \in S \tag{8.5}$$

$$y_i^{e,s} \geq \bar{y}_i^{e,s^d} \qquad \forall i \in E \tag{8.6}$$

$$n_{i0}^{e,s} = \bar{n}_{i0}^{e,s^d} \qquad \forall i \in E : \bar{y}_i^{e,s^d} = 1 \tag{8.7}$$

$$y_i^{e,l} = \bar{y}_i^{e,l^d} \qquad \forall i \in E \tag{8.8}$$

$$n_{i0}^{e,l} = \bar{n}_{i0}^{e,l^d} \qquad \forall i \in E : \bar{y}_i^{e,l^d} = 1 \tag{8.9}$$

$$n_{i0}^{r} \geq \bar{n}_{i0}^{r^d} \qquad \forall i \in R \tag{8.10}$$

Fig. 7 depicts robust designs, including locations and (initial) sizes of electrolysis plants and pipeline infrastructure as in the optimal robust solution, and deterministic designs, with repairs if needed, including locations and sizes of electrolysis plants and pipeline infrastructure as in the optimal deterministic solution, and the additional electrolysis plants and pipelines to repair the deterministic solution if the deterministic solution is not feasible in the uncertain environment, under different parameter settings. In the figure, electrolysis plants are represented by circles, CO_2 sources by squares, and syngas demand sites by triangles, and syngas transportation is represented by red lines and CO_2 transportation is represented by black lines. Additionally, the sizes of the circles are directly proportional to the sizes of the plants.

Figs. 7(a) and 7(b) are for Scenario 3, where $\boldsymbol{\gamma} = \mathbf{0.1}$ and PL-PU = 150–3000, while Figs. 7(c) and 7(d) are for Scenario 2, where $\boldsymbol{\gamma} = \boldsymbol{\gamma}^{\mathbf{T}}$ and PL-PU = 500–1850. Based on the figures, we can draw some implications related to the supply chain design. First, Figs. 7(a)

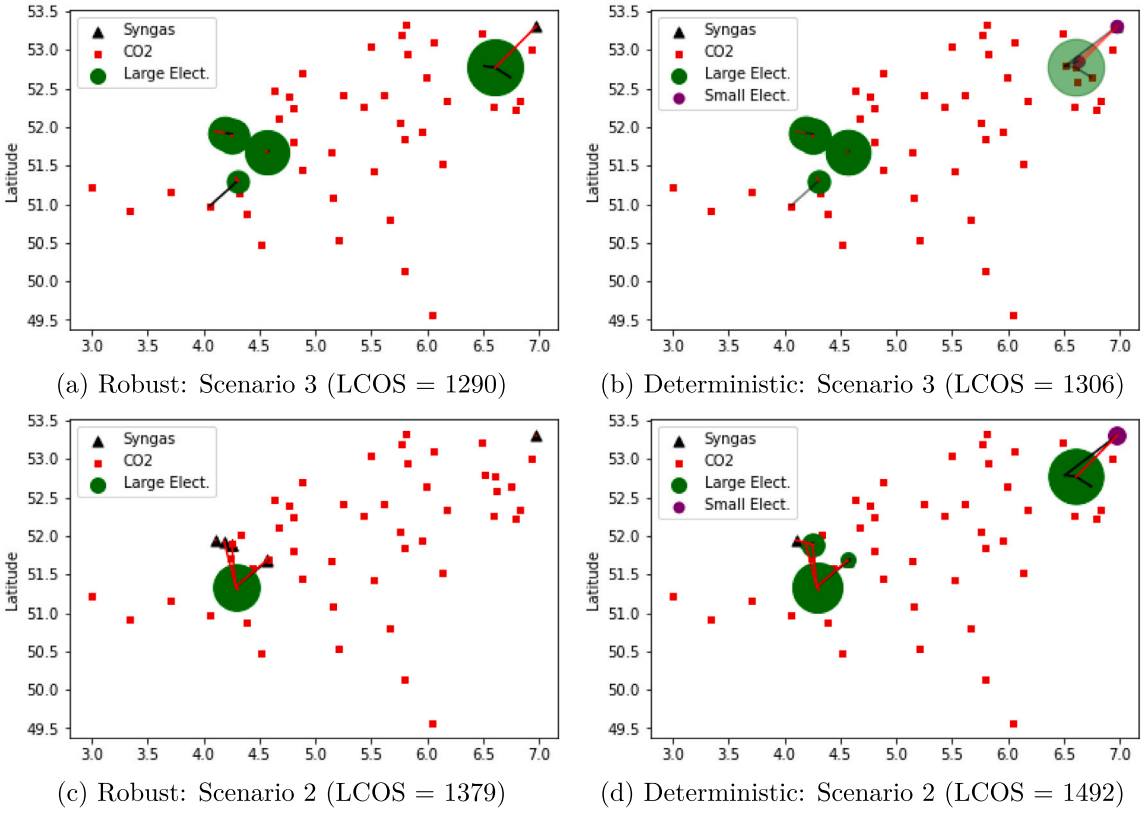

Fig. 7. Robust designs and deterministic designs (with repairs).

and 7(b) show that although strategic decisions such as the locations of large electrolysis plants are the same for both robust and deterministic solutions, the deterministic solution is not feasible in the uncertain environment because the determined sizes of the plants cannot satisfy demand requirements if the uncertainty is disregarded in the decision-making process. Note that if an electrolysis plant is located at a demand site, then its demand must be covered. Hence, to avoid infeasibility, two small-scale electrolysis plants are located and a new syngas pipeline is installed. If we compare the LCOS obtained by both designs, we see that the robust design provides 1.24% less LCOS. Second, Figs. 7(c) and 7(d) show that the number of large-scale electrolysis plants is also different in robust and deterministic designs. Unlike the deterministic design, the robust design chooses to cover half of the demand sites instead of all of them. Hence, the robust design can deal with the uncertainties in the demands and provide a positive profit. However, if the deterministic design is used in the uncertain environment, to compensate for all the cost of installed large-scale electrolysis plants, all demand sites are satisfied. As a result, a small-scale electrolysis plant is also located. Although all demand sites are covered, if the deterministic design is used, the profit becomes negative. Moreover, when we compare the LCOS obtained by both designs, we see that the robust design provides 8.19% less LCOS.

Table 1 shows the average of decreases, the maximum of the decreases, and the number of instances in which we observe there is a decrease in the LCOS when the robust solution is employed for the different scenarios. We can say that considering uncertainty is highly valuable for all scenarios. While the average decrease is the highest for Scenario 2, the maximum decrease of 22.23% is obtained for an instance of Scenario 3. It shows that decentralized planning is more vulnerable to uncertainties. Here, it is also important to highlight the importance of centralized planning for the supply chain design in terms of costs because when the LCOS obtained for Scenario 2 and Scenario 3 from robust solutions are compared, we see that Scenario 2, i.e., centralized planning for the Benelux countries, provides a design with 62.5% more profit and 6.29% less LCOS on average than the design obtained by Scenario 3, i.e., decentralized planning for the Benelux countries.

Table 1
The percentage decreases in the LCOS aggregated by scenarios.

Scenario	Average (%)	Max (%)	Number of Instances
1	1.36	4.60	13/15
2	5.23	16.78	15/16
3	5.09	22.23	15/16

Table 2 shows the average percentage decreases for price ranges and robustness parameters and the maximum percentage average decrease obtained for the given price ranges. It is seen that the value of considering uncertainty increases as the robustness parameter increases. Since, for some instances for the given robustness parameter and price ranges, it is not possible to obtain supply chain designs with the LCOS lower than the given PU, all feasible solutions have objective function values less than or equal to 0. In this case, the optimal decision becomes no production, and the model ends up with an optimal solution of 0. Accordingly, the LCOS becomes undefined due to a division by zero, as both the total cost and the quantity produced are zero in the case of no production. Hence, in the table, "–" represents there is not an instance, for three scenarios, with the optimal solution of a positive profit for the given robustness parameter and price range.

According to Table 2, the value of considering uncertainty increases as the robustness parameter increases, the price range decreases, and PU decreases. For the instances whose results are not reported in the table, we explore how much the upper price limit must be increased to obtain a positive profit. Hence, PU is incrementally increased from 1600 to 2100 in steps of 100. The minimum PU value that provides

Table 2
Average percentage decreases in the LCOS.

PL-PU	γ							Max
	0.1	**0.15**	**0.2**	**0**.25	**0.3**	γ^T	γ^S	
150–1500	2.45	14.09	–	–	–	–	1.53	16.43
500–1850	2.81	2.55	5.13	13.66	–	4.29	3.85	22.23
150–3000	0.93	1.82	2.50	3.06	3.78	1.27	1.16	4.88

Table 3
Optimal robust LCOS and price for increased PU values for Scenario 1 instances.

PL	γ	PU	LCOS	Price of syngas
150	**0.15**	1600	1466	1511
150	**0.2**	1700	1617	1636
150	**0.25**	1900	1794	1828
150	**0.3**	2100	1997	2020
150	γ^T	1700	1605	1636
500	**0.3**	2100	1972	2002

Table 4
CPU times (in seconds) for deterministic and robust formulations.

Scenario	PL-PU	Deterministic formulation (4)	Robust formulation (7)
1	150–1500	44	115
	500–1850	28	622
	150–3000	27	29
2	150–1500	963	1100
	500–1850	342	1106
	150–3000	119	295
3	150–1500	18	42
	500–1850	10	76
	150–3000	21	15

an optimal solution with positive production decisions for each instance in Scenario 1 is reported in Table 3. The table shows that the required increase in PU heavily depends on the robustness parameter, i.e., higher uncertainty levels require greater increases, as observed for the instances with PL of 150. Furthermore, when analyzing the instances with the robustness parameter of **0.3**, it is seen that PU must be 2100 for both PL of 150 and 500, indicating increases of 600 and 250, respectively. Since the resulting PU values are the same, this shows that a smaller price range can lead to lower prices and LCOS.

We assess the computational efficiency of the proposed robust model in terms of CPU time, which is the total time spent to solve the problem. To this end, we compare the solution times of the deterministic and robust formulations for the same instances with the same scenario and price range settings. The CPU time for solving the robust formulation is reported as the average over different robustness parameters. Table 4 presents the results and shows that the robust formulation provides optimal solutions within a reasonable time for each instance.

3.3. Cost analyses for different settings for the key factors

The effects of government financial support

In this part, we investigate the effects of different government financial support levels for Scenario 1 and Scenario 2 by analyzing the changes in the price and LCOS, the shares of the costs in the LCOS, and the designs including the locations and sizes of the electrolysis plants and the pipeline infrastructure. Fig. 8 shows how the LCOS and price change as the level of financial support changes. Note that financial support is considered as a percentage reduction in CAPEX and OPEX. Fig. 9 shows the shares of the costs in the LCOS for Scenario 1 and Scenario 2 instances, where the costs are categorized for CO_2 capture technologies, CO_2 and syngas pipeline infrastructure, battery installations, electrolyzer installations including stack replacements, renewable electricity generation, water consumption, and the electricity consumption from the grid. Figs. 10 and 11 show the designs for Scenario 1 and Scenario 2 instances under four different levels of government financial support.

In Fig. 8, as the level of financial support increases, the price and LCOS generally decrease. We only observe an increase in the LCOS for Scenario 2 when the government financial support level is 0.1. The reason is that, when the level increases from 0 to 0.1, as Fig. 11(b) shows, it becomes profitable to cover the biggest demand site which is in the north of the Netherlands. From Fig. 9, it can be inferred that the share of infrastructure costs is higher for Scenario 2 than Scenario 1 because, since the carbon footprint level of the grid in Belgium is better than the one in the Netherlands, the electrolysis plant with a high capacity is located in Belgium and syngas demand in the Netherlands is satisfied from this plant, which requires installing pipelines for syngas transportation. This is clearly seen in Figs. 10 and 11, especially if the support level is less than 0.8. It can be said that as the government financial support level increases, the designs for both scenarios are becoming similar to each other because when investing in renewable sources becomes more affordable, the effect of the grid characteristics on the solutions decreases. Hence, the differences between the designs for both scenarios mainly resulted from the effect of avoiding making huge investments in renewable energy sources.

In Fig. 9, for support level of 0.6 for Scenario 1, a small share of the LCOS is spent on battery installations to the electrolyzer located closer to the big demand site in the north of the Netherlands. This shows that when batteries become more affordable, they will be firstly preferred by the largest electrolysis plants. The figure also shows that, for both scenarios at the support level of 0.8, the cost of using a unit of renewable electricity becomes cost-competitive with the cost of using electricity from the grid. Hence, the capacity of renewable electricity investments increases together with the electrolyzer capacities and almost 100% of renewable electricity is used at the electrolysis plants.

As it is seen in Fig. 8, when the financial support level increases, the profit margin also increases. If the price is aimed to be set under some level, an additional constraint can be used. For example, if the nominal demand is desired to be at least half of the base demand, then the following constraint

$$\sum_{l \in L} pr_l \rho_l \leq 1500 \tag{9}$$

can be added to Formulation (7). Respectively, if we solve instances for Scenario 1 under different support levels, the price of syngas and LCOS will change as shown in Fig. 12. According to the figure, until the support level of 0.4, it is not possible to have a positive profit; at the support level of 0.4, LCOS of 1480 can be obtained instead of 1528; for the support levels larger than 0.4, the LCOS is similar to the ones obtained without using Constraint (9). With this constraint, for the support level of 0.4, less LCOS is obtained. However, when the optimal solutions are analyzed for two different cases of with and without the constraint, as can be seen in Fig. 13, fewer demand sites are served, i.e, 98% less demand is covered in total if an additional limit on the price is set.

The effects of battery usage

In the computational results previously reported, except for the instance of Scenario 1 under the government financial support level of 0.6, batteries are not used at electrolysis plants. This is because using batteries can be extremely expensive due to their high investment costs and degradation rates. Instead of installing batteries, the capacities of electrolyzers are increased, allowing more tonnes of syngas to be produced within fewer operating hours, mostly during the available supply of direct renewable electricity. In this part, we analyze different cases that can favor battery usage.

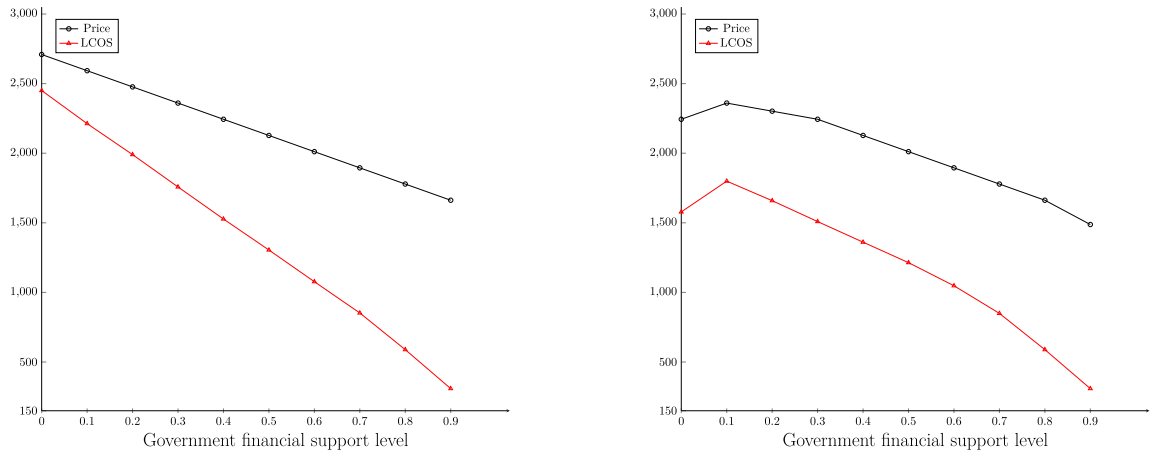

Fig. 8. Price of syngas and LCOS under different government financial support levels.

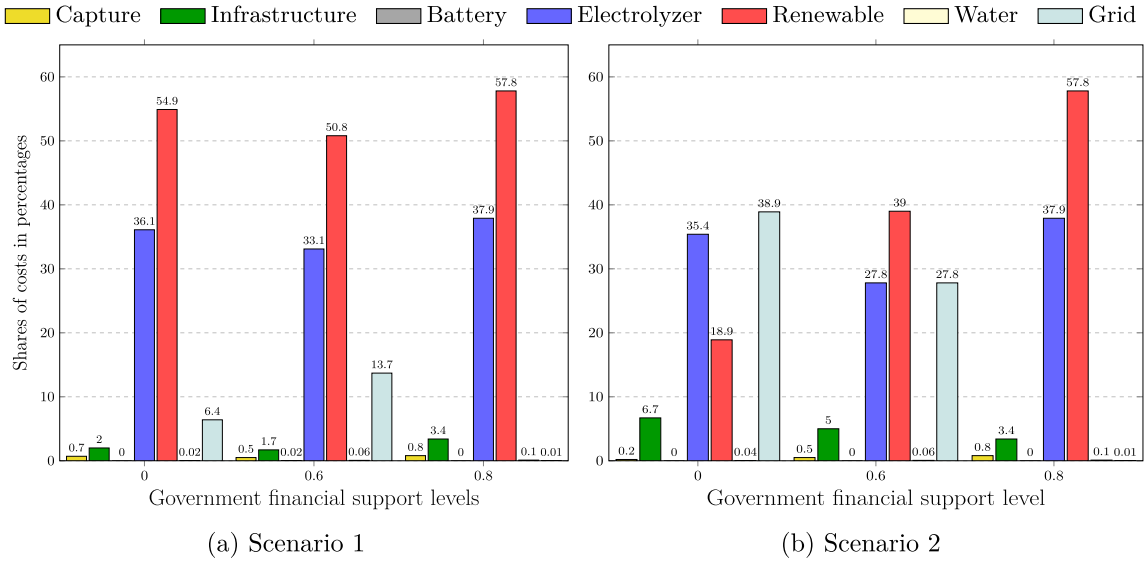

Fig. 9. Shares of costs in the LCOS under different levels of government financial support.

We investigate the cases where there are additional financial supports for the CAPEX of battery installations in addition to the government financial supports for every CAPEX in the system. When we analyze different additional support levels, we see that batteries start to be employed if there is an additional support level of 0.36 and 0.15 for the battery in Scenarios 1 and 2, respectively. Fig. 14 shows how the LCOS and total battery capacity change if different levels of additional financial support are used. For Scenario 2, although batteries are employed for the additional support levels of greater than or equal to 0.15, until the level of 0.35, batteries are used only at the electrolysis plant in the north of the Netherlands. The reason is that this electrolyzer serves the biggest demand site, and it is located in the Netherlands whose grid has a relatively larger carbon footprint. After the level of 0.35, batteries start to be used at all electrolysis plants, and we observe similar behavior for decreases in the LCOS for both Scenarios 1 and 2. To see changes in the cost shares of LCOS for additional support levels of 0 and 0.36 for scenarios, Fig. 15 is provided. In the figure, it can be clearly seen that there is a trade-off between the capacities of electrolyzers and batteries because, with increasing additional financial support levels for both scenarios, the share of battery costs increases and the share of electrolyzer costs decreases, while the shares of all other cost components remain nearly unchanged.

We also analyze the case where electrolyzers operate continuously for 8000 hours per year. Due to the inequality in Constraint (3.20), we allow operating hours less than or equal to 8000 per year. As a result, at the electrolysis plants, the production is usually done during the direct renewable electricity supply, e.g., 4000 hours, and during a small portion of the remaining 4000 hours with electricity from the grid. Consequently, annual demand of customers is generally produced within a half-year operation at the electrolysis plants. However, customers may prefer a more evenly distributed syngas supply throughout the year. In this case, Constraint (3.20) can be rewritten as an equality. When the equality constraint is used, the LCOS decreases from 1748 to 1309 for Scenario 1 if the level of additional financial support for batteries is changed from 0 to 0.36, while the LCOS decreases from 1401 to 1329 for Scenario 2 if the level of additional financial support for batteries is changed from 0 to 0.15. As seen in Fig. 16, when there is no additional financial support for batteries, the share of battery costs constitutes one of the largest cost components for both scenarios, especially for Scenario 1, it is the second largest cost component because the employment of batteries is more important to increase the utilization of renewable electricity because the grid has a larger carbon footprint. Fig. 17 depicts how designs change for Scenario 1 and

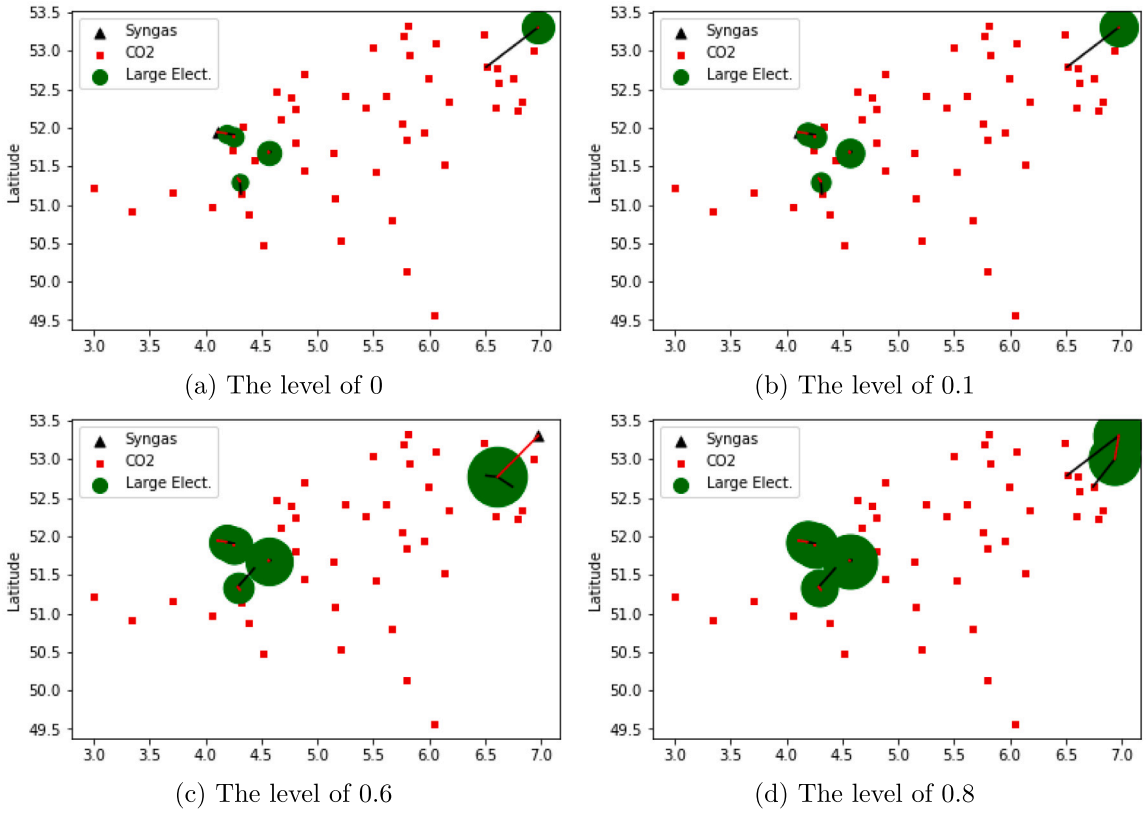

Fig. 10. Designs under different levels of government financial support for Scenario 1.

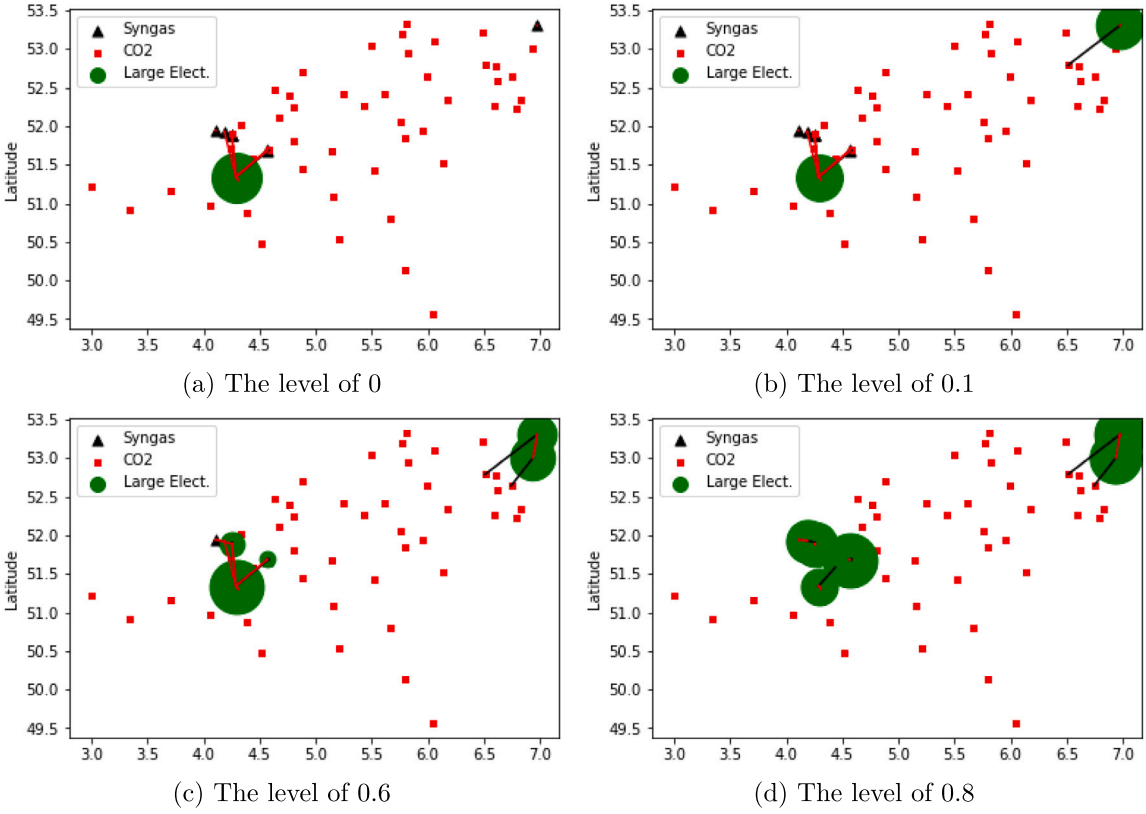

Fig. 11. Designs under different levels of government financial support for Scenario 2.

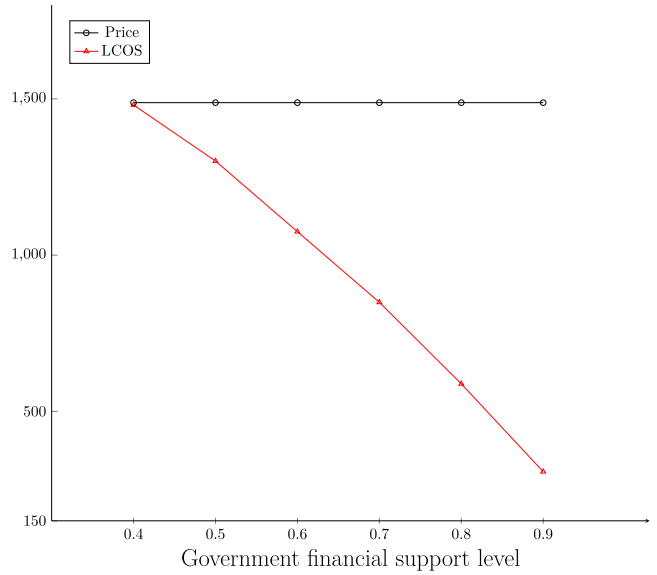

Fig. 12. Price of syngas and LCOS for Scenario 1 with an additional constraint of Constraint (9).

Scenario 2 for additional support levels for batteries. In Scenario 1, if there is an additional support of 0.36, the price can be chosen lower due to smaller LCOS, and thus the demands increase at demand sites and the total capacities of electrolyzers increase. Furthermore, since the increase in demand is the greatest for the demand site in the north of the Netherlands, the location of the electrolysis plant that serves it changes, and the plant is opened closer to the CO_2 sources. When we analyze the changes for Scenario 2, it is seen that the same price is chosen, and thus the same demands are observed. The number of large-scale electrolysis plants and their capacities decreases as a result of higher operating hours with the help of batteries, and two small electrolysis plants with batteries are installed in the Netherlands, which leads to decreases in infrastructure costs. The decrease in infrastructure costs can also clearly be seen in Fig. 16 for Scenario 2.

The effects of variability in the renewable electricity supply

The level of variability determines how many hours in a year the electrolysis plants can directly use renewable electricity. For example, when the maximum operation hour is 8000 hours, if the variability level is 0.3, then there is a direct renewable electricity supply in 5600 hours; if the variability level is 0.5, then there is a direct renewable electricity supply in 4000 hours; if the variability level is 0.7, then there is a direct renewable electricity supply in 2400 hours. Hence, as the variability level increases, the number of hours in which renewable electricity can be directly used decreases.

Fig. 18 shows how the price and LCOS change as the variability increases. For both scenarios, the price and LCOS increase in a similar manner as the variability level increases. A higher level of variability results in a larger number of electrolysis plants and higher capacities to compensate for the reduced availability of renewable electricity supply. As seen in Fig. 19, the share of electrolyzers also increases for both scenarios. Since the costs of other components change only slightly across different variability levels, the shares of these components in the LCOS decrease as the share of electrolyzer costs increases significantly, especially for Scenario 1. Additionally, it is important to note that the role of batteries becomes more significant as the variability increases. Specifically, for Scenario 1, we observe that when the level of variability is 0.7, the batteries start to be installed with the electrolyzers if the additional financial support is 0.2 instead of 0.36, which is the least additional financial support level when the variability level is 0.5.

4. Conclusion

In this work, we introduce a multi-period supply chain design problem for CO_2-based syngas under demand uncertainty and propose a mixed integer linear programming robust model to solve it. The significant uncertainties in governance and financial factors highlight the necessity of incorporating uncertainty into the supply chain design. Given both market uncertainties and the influence of governance and financial factors on demand, we integrate demand uncertainty into the decision-making process. We employ an interval-based model for future demand realizations, which provides information regarding the lowest and highest possible demand realizations depending on the chosen price. The nonlinearities arising from the dependencies between variables are linearized to ensure model tractability.

We constrain the global warming potential of the electricity consumed during syngas production to contribute to environmental feasibility. Since electrolysis is highly electricity intensive, careful planning of electricity consumption is essential. To increase the use of renewable electricity, we consider an integrated electricity supply system consisting of the grid, renewable resources and batteries, whose capacities are determined as supply chain decisions. For economic feasibility, our objective is to maximize the net present value of the entire investment plan for the supply chain. Consequently, with the proposed robust model that considers financial, environmental, and governance aspects, we guarantee the applicability of the supply chain design under all possible demand realizations and the best performance under worst-case demand realizations.

We generate data using the Delphi method, sources from the literature, and available technical reports and implement the proposed model on the Benelux region using the data. We conduct computational experiments under varying settings. Based on the results obtained, we derive managerial insights that highlight the importance of incorporating uncertainty, improving renewable electricity use, balancing infrastructure investments, and understanding the impact of financial support. First, considering the demand uncertainty can significantly affect decisions because disregarding it can lead to higher LCOS and negative profits, both of which hinder the adoption and future of CO_2-based syngas due to low customer satisfaction and low interest from financial investors. For example, incorporating the demand uncertainty into the decision-making process can lower the average LCOS by up to 14%, with a maximum reduction of 22%. Second, the investment in renewable electricity generation is the primary cost driver because its share in the LCOS is typically the highest. Hence, strategic decisions are strongly influenced by grid characteristics. A high penetration of renewable sources in the grid is significantly favored by electrolysis plant location decisions, leading to longer pipeline installations. A higher level of government financial support can eliminate differences in strategic decisions due to different grid characteristics. For example, a 33% increase in the government financial support level can decrease infrastructure investments by up to 62%. Additionally, when the level of financial support is 80%, electrolysis plants can use 100% renewable electricity in the production of syngas. Third, there exists a trade-off between battery and electrolyzer installations. Regardless of grid characteristics, an additional financial support of 30% for battery installations can reduce electrolyzer installations by doubling the operating hours of electrolysis plants. In case of no additional financial support, battery installations become essential when continuous production is required because they are necessary to meet the desired global warming potential of electricity consumption. Additionally, battery installations help deal with the renewable electricity supply variability, whose 40% increase can increase electrolyzer installation costs by up to 67%. Lastly, government financial support plays a key role in lowering product prices and LCOS, where the LCOS decreases in a greater magnitude than the price while the financial support level

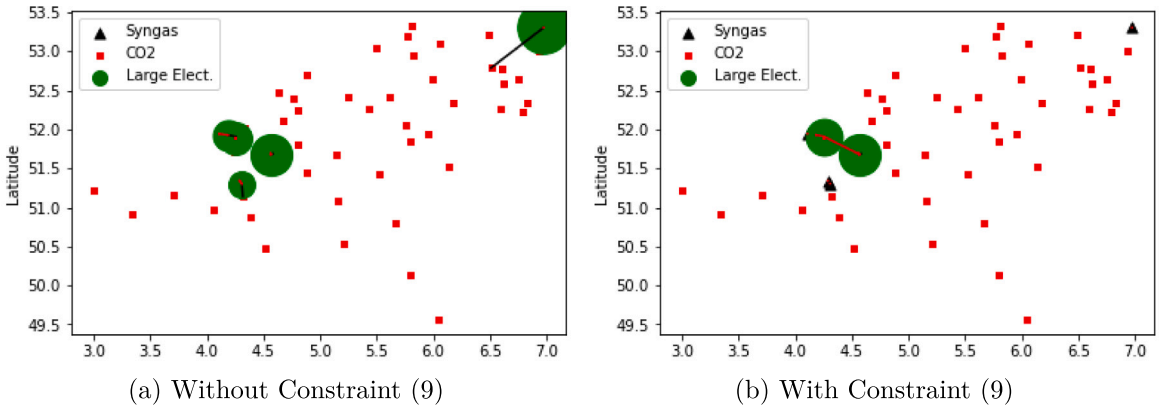

Fig. 13. Designs under financial support level of 0.4 for Scenario 1 with and without Constraint (9).

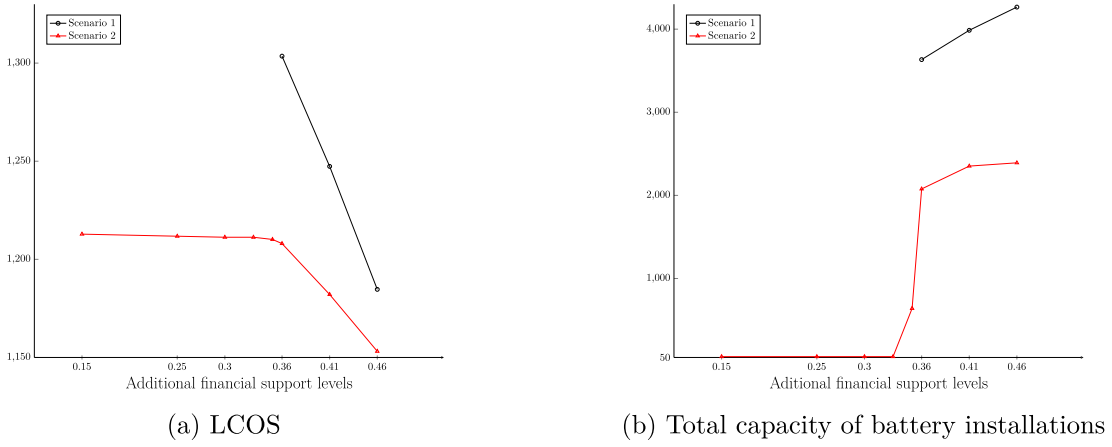

Fig. 14. LCOS and battery capacity under different levels of additional financial support.

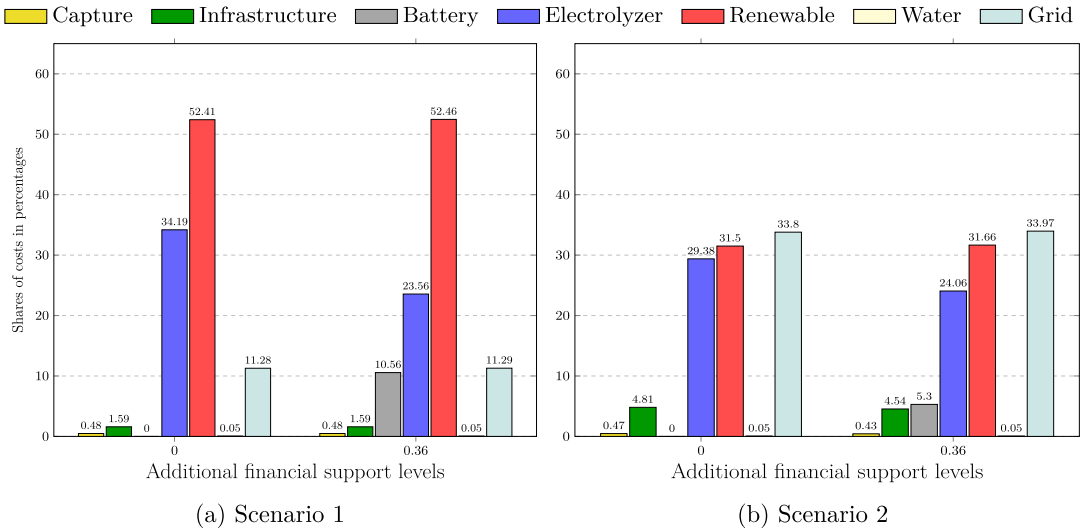

Fig. 15. Shares of costs in the LCOS under different levels of additional financial support.

increases. Higher levels of financial support allow the scaling up of CO_2-based syngas deployment in its early stages because lower product prices lead to higher demand realizations at demand sites, whereas reduced investment costs enable the employment of a greater number of electrolysis plants with larger capacities to serve a greater number of larger demand sites.

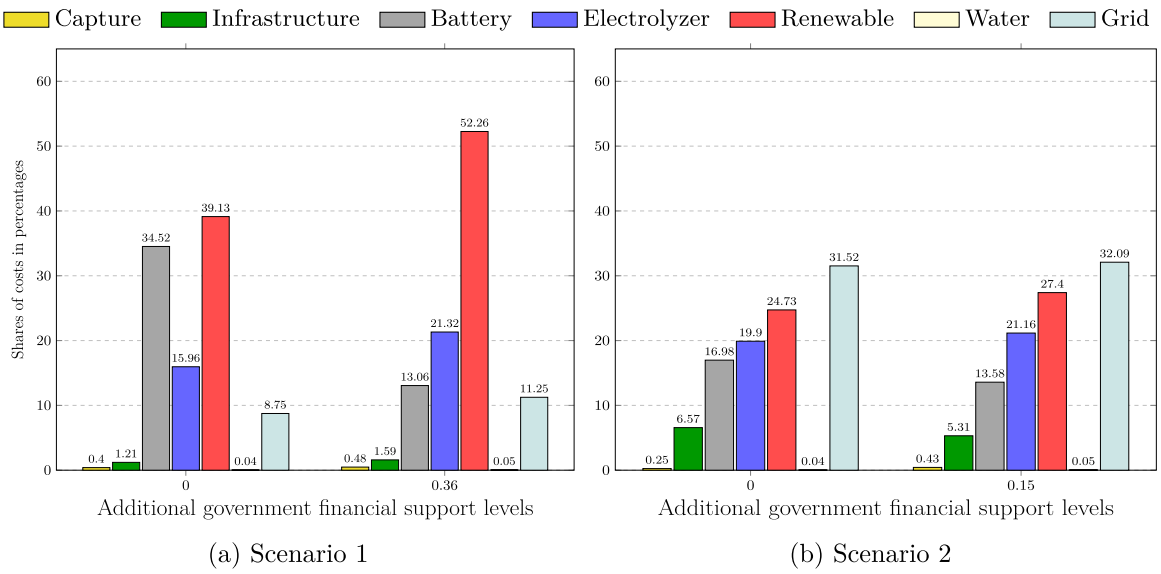

Fig. 16. Shares of costs in the LCOS under different additional financial support levels for the continuous production.

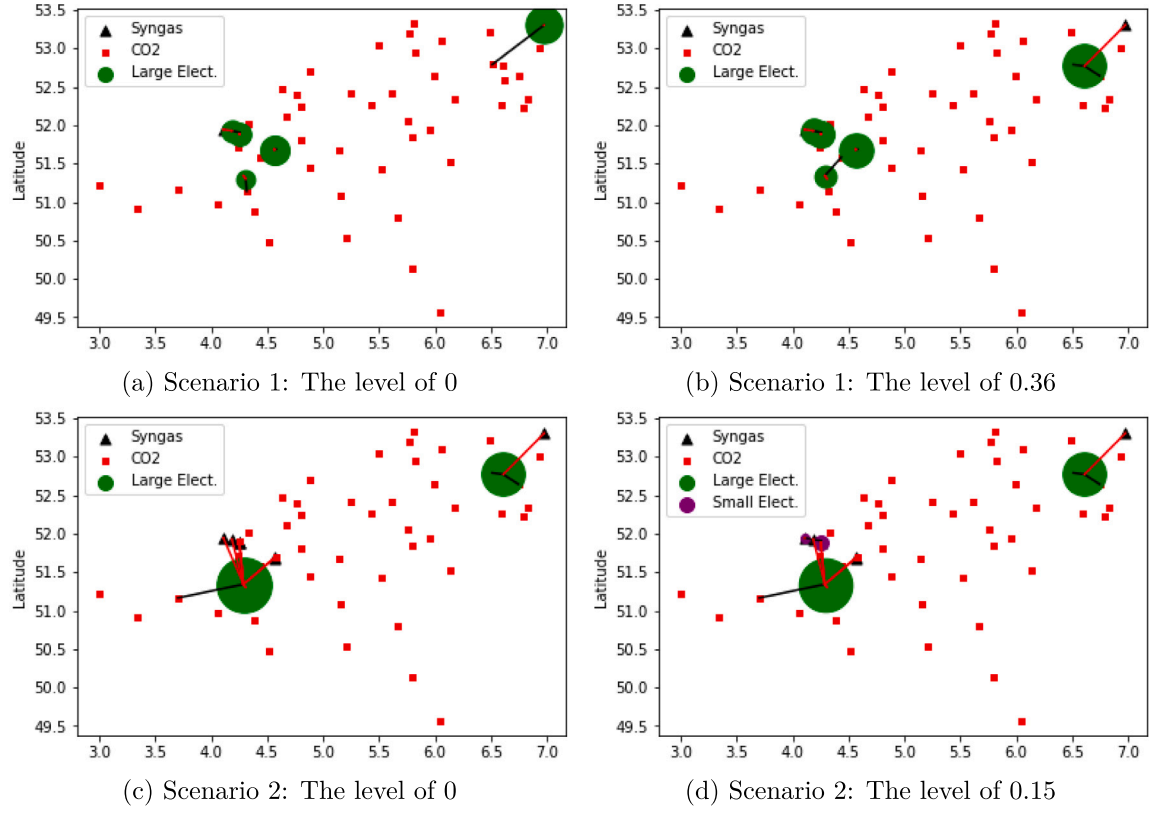

Fig. 17. Designs under different additional financial support levels for the continuous production.

There are several future research directions. First, while we analyze demand uncertainty and its relation to costs and governance, uncertainties in multiple parameters can be explored in future studies. Second, since supply chain design involves long-term strategic decisions, we aggregate production annually for consistency. Future research can optimize production at a specific electrolysis plant on a daily or hourly basis, accounting for renewable electricity intermittency. Third, since electricity consumption significantly impacts the global warming potential of CO_2-based syngas, we use carbon emission constraints. To fully assess the competitiveness of CO_2 electrolysis against other sustainable technologies, like biomass gasification, a cradle-to-grave life cycle assessment should be used.

CRediT authorship contribution statement

Özlem Mahmutoğulları: Writing – review & editing, Writing – original draft, Visualization, Validation, Software, Resources, Methodology, Investigation, Formal analysis, Data curation, Conceptualization. **Nevin Mutlu:** Writing – review & editing, Writing – original draft,

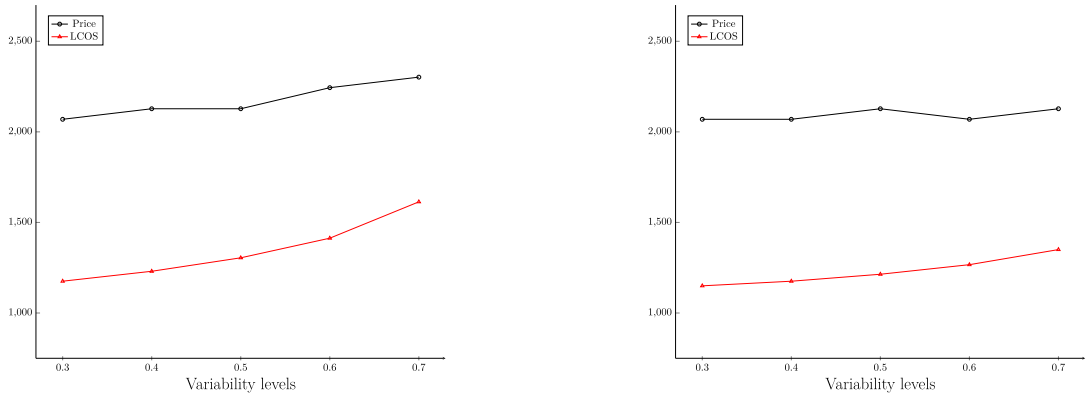

Fig. 18. Price of syngas and LCOS under different levels of variability in renewable electricity.

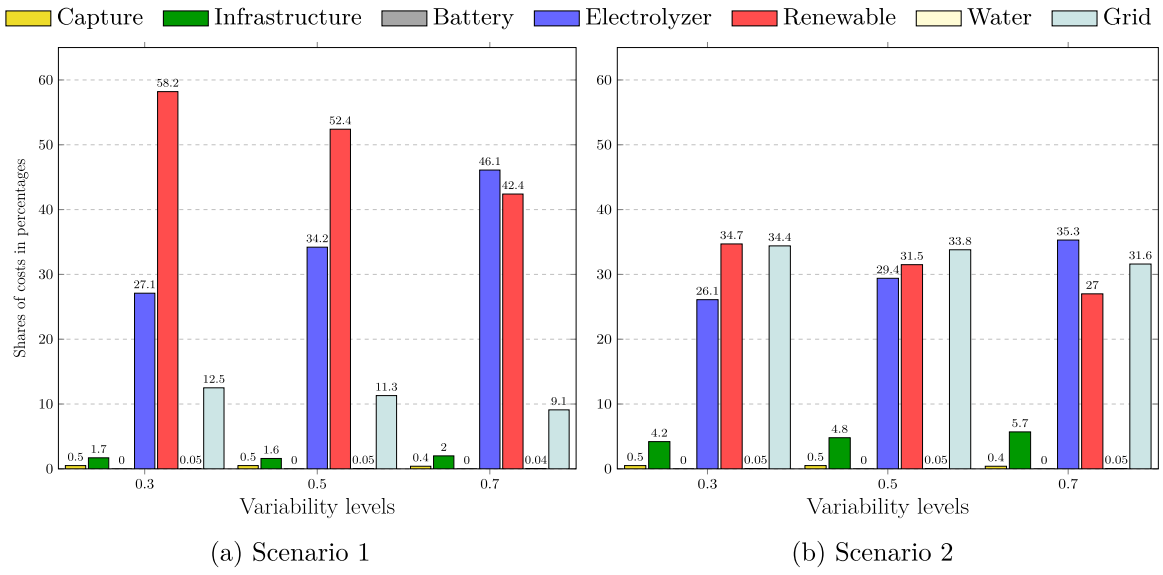

Fig. 19. Shares of costs in the LCOS under different levels of variability in renewable electricity.

Supervision, Methodology, Conceptualization. **Tarkan Tan:** Writing – review & editing, Writing – original draft, Supervision, Methodology, Conceptualization. **Mar Pérez-Fortes:** Writing – review & editing, Writing – original draft, Supervision, Resources, Project administration, Methodology, Funding acquisition, Data curation, Conceptualization.

Funding sources

This research is part of the project "Sustainable design of multi-scale CO_2 electrochemical conversion" (with project number ECCM.TT.MVITU.006) of the electro-chemical conversion materials and responsible innovation (ECCM MVI) top-up program which is (partly) financed by the Dutch Research Council (NWO).

Declaration of competing interest

The authors declare that they have no known competing financial interests or personal relationships that could have appeared to influence the work reported in this paper.

Acknowledgments

We thank the voluntary collaboration and contributions of the participants in the questionnaires and workshop "CO_2 electrolysis (CO_2E) workshop" (held in Delft, the Netherlands on April 25, 2024). Thanks to the research team (Josephine Vos, Thijmen Wiltink, Sanghamitra Chakravarty, Ibo van de Poel, Hans de Bruijn, Tarkan Tan and Nevin Mutlu) for their help in the conception and organization of the workshop, and to Marula Tsagkari for her organizational role. Thanks to Thijmen Wiltink for his provision of part of the data and to Floor Alkemade for her valuable insights in the conception of this work. During the preparation of this paper the authors used ChatGPT (OpenAI, 2025) in order to check grammar, spelling, and sentence structure. After using this tool, the authors reviewed and edited the content as needed and take full responsibility for the content of the publication.

Appendix

See Table 5.

Data availability

Data can be accessed at https://edu.nl/bpxfh.

Table 5
Descriptions of notations for sets, parameters, and decision variables.

	Descriptions	Units
Sets		
C	Set of CO_2 sources	
S	Set of syngas demand sites	
E	Set of potential locations for CO_2 electrolysis plants	
L	Set of price settings for CO_2-based syngas	
R	Set of zones for electricity consumption	
T	Set of time periods	
Parameters		
d_{it}^{base}	Base annual demand for syngas at syngas demand site $i \in S$ in period $t \in T$	tonne
d_{itl}	Annual demand for syngas at syngas demand site $i \in S$ in period $t \in T$ under price level $l \in L$	tonne
$\bar{d}_{itl}$	Nominal annual demand for syngas at syngas demand site $i \in S$ in period $t \in T$ under price level $l \in L$	tonne
γ_{it}	Percentage deviation from nominal demand of syngas demand site $i \in S$ in period $t \in T$	–
f^s	Cost of pipeline infrastructure for syngas transportation	EUR/km
f^c	Cost of pipeline infrastructure for CO_2 transportation	EUR/km
f_i^{cap}	Cost of using a CO_2 capture technology at CO_2 source $i \in C$	EUR
g_i^c	The annual amount of CO_2 at CO_2 source $i \in C$	tonne
d_{ij}^{ce}	Distance between CO_2 source $i \in C$ and electrolysis plant $j \in E$	km
d_{ij}^{es}	Distance between electrolysis plant $i \in E$ and syngas demand site $j \in S$	km
h	The annual operating hours of electrolysis plants	h
U^i	The maximum capacity for an electrolysis plant with scale $i \in \{s,l\}$	MW
L^i	The minimum capacity for an electrolysis plant with scale $i \in \{s,l\}$	MW
M^c	The maximum distance allowed for CO_2 transportation between two sites	km
M^s	The maximum distance allowed for syngas transportation between two sites	km
M	A large number	–
exC	The maximum percentage capacity increase allowed in each period	–
l^b	Percentage capacity loss (degradation) in each unit of capacity for batteries per period	–
$\kappa_t^{e,i}$	Capital cost of capacity for electrolysis plants with scale $i \in \{s,l\}$ in period $t \in \{T \cup \{0\}\}$	EUR/MW
$\omega_t^{e,i}$	Annual operational cost of capacity for electrolysis plants with scale $i \in \{s,l\}$ in period $t \in \{T \cup \{0\}\}$	EUR/MW
ψ_t^i	Stack replacement cost for electrolysis plants with scale $i \in \{s,l\}$ in period $t \in T$	EUR/MW
κ_t^r	Capital cost of capacity for renewable electricity generation plants in period $t \in \{T \cup \{0\}\}$	EUR/MW
ω_t^r	Annual operational cost of capacity for renewable electricity generation plants in period $t \in \{T \cup \{0\}\}$	EUR/MW
κ_t^b	Capital cost of capacity for batteries in period $t \in \{T \cup \{0\}\}$	EUR/MW
ω_t^b	Annual operational cost of capacity for batteries in period $t \in \{T \cup \{0\}\}$	EUR/MW
I	Interest rate	–
a^c	CO_2 required for producing per tonne of syngas	tonne
a^e	Electricity required for producing per tonne of syngas	MWh
a^w	Water required for producing per tonne of syngas	tonne
p^w	Price of water	EUR/tonne
p_t^e	Price of grid electricity in period $t \in T$	EUR/MWh
η_{it}	Share of renewable sources in grid in zone $i \in R$ in period $t \in T$	–
μ_{it}	Capacity factor for the renewable electricity supply in zone $i \in R$ in period $t \in T$	–
ν	Percentage variability in renewable electricity supply	–
GWP_i^r	Carbon footprint of electricity generated from renewable sources in zone $i \in R$	kg CO_2-eq/MWh
GWP_i^{non-r}	Carbon footprint of electricity generated from non-renewable sources in zone $i \in R$	kg CO_2-eq/MWh
GWP_{it}^g	Carbon footprint of grid electricity in zone $i \in R$ in period $t \in T$	kg CO_2-eq/MWh
pr_l	Price of CO_2-based syngas under price setting $l \in L$	EUR/tonne syngas
PL	Minimum price of CO_2-based syngas	EUR/tonne syngas
PU	Maximum price of CO_2-based syngas	EUR/tonne syngas
u^{gwp}	Maximum unit carbon footprint of electricity consumed during production allowed	kg CO_2-eq/tonne syngas
o_{ij}	1 if electrolysis $i \in E$ plant is located in the zone $j \in R$; 0 otherwise	–
o_{ij}^e	1 if electricity transmission is allowed between zones $i, j \in R$; 0 otherwise	–
Decision variables		
$y_i^{e,j}$	1 if an electrolysis plant with scale $j \in \{s,l\}$ is located at potential location $i \in E$; 0 otherwise	–
y_i^c	1 if a CO_2 capture technology is used at CO_2 source $i \in C$; 0 otherwise	–
z_{it}	1 if syngas demand site $i \in E$ is covered in period $t \in T$; 0 otherwise	–
ρ_l	1 if price of syngas is selected at level $l \in L$; 0 otherwise	–
ζ_{itl}	1 if $z_{it} = 1$ and $\rho_l = 1$ for $i \in E$, $t \in T$, $l \in L$; 0 otherwise	–
θ_{ij}^c	1 if pipeline is installed between CO_2 source $i \in C$ and electrolysis plant $j \in E$; 0 otherwise	–
θ_{ij}^s	1 if pipeline is installed between electrolysis plant $i \in E$ and syngas demand site $j \in S$; 0 otherwise	–
$n_{it}^{e,j}$	Annual capacity of electrolysis plant with scale $j \in \{s,l\}$ at location $i \in E$ in period $t \in T$	MW
n_{it}^r	Annual capacity of renewable electricity plant in zone $i \in R$ in period $t \in T$	MW
n_i^b	Annual capacity of batteries at location $i \in E$ in period $t \in T$	MW
q_{it}^c	Annual amount of CO_2 captured at CO_2 source $i \in C$ in period $t \in T$	tonne
q_{it}^s	Annual amount of syngas produced at electrolysis plant $i \in E$ in period $t \in T$	tonne
e_{it}^g	Annual amount of grid electricity used at electrolysis plant $i \in E$ in period $t \in T$	MWh
e_{it}^r	Annual amount of renewable electricity used at electrolysis plant $i \in E$ in period $t \in T$	MWh
e_{it}^b	Annual amount of renewable electricity stored in battery at electrolysis plant $i \in E$ in period $t \in T$	MWh
x_{ijt}^c	Annual amount of CO_2 sent from CO_2 source $i \in C$ to electrolysis plant $j \in E$ in period $t \in T$	tonne
x_{ijt}^s	Annual amount of syngas sent from electrolysis plant $i \in E$ to syngas demand site $j \in S$ in period $t \in T$	tonne

References

Ardjmand, E., Weckman, G.R., Young, W.A., Sanei Bajgiran, O., Aminipour, B., 2016. A robust optimisation model for production planning and pricing under demand uncertainty. Int. J. Prod. Res. 54 (13), 3885–3905.

Bachmann, M., Völker, S., Kleinekorte, J., Bardow, A., 2023. Syngas from what? Comparative life-cycle assessment for syngas production from biomass, CO_2, and steel mill off-gases. ACS Sustain. Chem. Eng. 11 (14), 5356–5366.

Chinneck, J.W., Ramadan, K., 2000. Linear programming with interval coefficients. J. Oper. Res. Soc. 51 (2), 209–220.

Clean Energy Technology Observatory, 2023. Wind energy in the European Union - 2023 status report on technology development, trends, value chains and markets. Retrieved from https://publications.jrc.ec.europa.eu/repository/handle/JRC135020. (Accessed 9 January 2025).

Clean Energy Technology Observatory, 2024. Battery technology in the European Union - 2024 status report on technology development, trends, value chains and markets. Retrieved from https://op.europa.eu/en/publication-detail/-/publication/036cd3d7-a55d-11ef-85f0-01aa75ed71a1/language-en. (Accessed 9 January 2025).

d'Amore, F., Romano, M.C., Bezzo, F., 2021. Carbon capture and storage from energy and industrial emission sources: A Europe-wide supply chain optimisation. J. Clean. Prod. 290, 125202.

Detz, R.J., Ferchaud, C.J., Kalkman, A.J., Kemper, J., Sánchez-Martínez, C., Saric, M., Shinde, M.V., 2023. Electrochemical CO_2 conversion technologies: State-of-the-art and future perspectives. Sustain. Energy Fuels 7 (23), 5445–5472.

Dittrich, L., Nohl, M., Jaekel, E.E., Foit, S., de Haart, L.B., Eichel, R.-A., 2019. High-temperature co-electrolysis: A versatile method to sustainably produce tailored syngas compositions. J. Electrochem. Soc. 166 (13), F971.

European Commission, 2019. Electricity interconnections with neighbouring countries: Second report of the commission expert group on interconnection targets. Retrieved from https://op.europa.eu/en/publication-detail/-/publication/785f224b-93cd-11e9-9369-01aa75ed71a1. (Accessed 10 January 2025).

European Commission, 2024a. Towards an ambitious industrial carbon management for the EU. Retrieved from https://eur-lex.europa.eu/legal-content/EN/TXT/PDF/?uri=CELEX:52024DC0062. (Accessed 20 August 2024).

European Commission, 2024b. Solar energy. Retrieved from https://energy.ec.europa.eu/topics/renewable-energy/solar-energy_en. (Accessed 7 March 2025).

European Commission, 2024c. EU wind energy. Retrieved from https://energy.ec.europa.eu/topics/renewable-energy/eu-wind-energy_en. (Accessed 7 March 2025).

European Council, 2024. Paris agreement on climate change. Retrieved from https://www.consilium.europa.eu/en/policies/climate-change/paris-agreement/. (Accessed 9 July 2024).

European Industrial Gases Association, 2022. Carbon monoxide and syngas pipeline systems. Retrieved from https://www.eiga.eu/uploads/documents/DOC120.pdf. (Accessed 25 June 2024).

European Network of Transmission System Operators for Electricity, 2021. Bidding zone configuration technical report 2021. Retrieved from https://www.entsoe.eu/news/2021/11/18/entso-e-publishes-its-2021-bidding-zone-technical-report-providing-a-transparent-and-factual-information-on-grid-congestions-in-the-eu/. (Accessed 4 March 2025).

European Parliment, 2023a. Scientific foresight: What if?: What if the EU were energy independent? Retrieved from https://www.europarl.europa.eu/RegData/etudes/ATAG/2023/753182/EPRS_ATA(2023)753182_EN.pdf. (Accessed 4 March 2025).

European Parliment, 2023b. EU rules for renewable hydrogen: Delegated regulations on a methodology for renewable fuels of non-biological origin. Retrieved from https://www.europarl.europa.eu/RegData/etudes/BRIE/2023/747085/EPRS_BRI(2023)747085_EN.pdf. (Accessed 10 January 2025).

Eurostat, 2023a. Use of renewables for electricity - details. Retrieved from https://ec.europa.eu/eurostat/databrowser/view/nrg_ind_ured/default/table?lang=en. (Accessed 24 February 2024).

Eurostat, 2023b. Gross and net production of electricity and derived heat by type of plant and operator. Retrieved from https://ec.europa.eu/eurostat/databrowser/view/nrg_ind_peh/default/table?lang=en. (Accessed 24 February 2024).

Eurostat, 2024a. Electricity production capacities for renewables and wastes. Retrieved from https://ec.europa.eu/eurostat/databrowser/product/page/NRG_INF_EPCRW. (Accessed 13 December 2024).

Eurostat, 2024b. Use of renewables for electricity - Details. Retrieved from https://ec.europa.eu/eurostat/databrowser/view/nrg_ind_ured$defaultview/default/table?lang=en. (Accessed 13 December 2024).

Eurostat, 2024c. Electricity prices for non-household consumers - Bi-annual data (from 2007 onwards). Retrieved from https://ec.europa.eu/eurostat/databrowser/view/nrg_pc_205_custom_14668276/default/table?lang=en. (Accessed 13 December 2024).

Eurostat, 2024d. Electricity price statistics. Retrieved from https://ec.europa.eu/eurostat/statistics-explained/index.php?title=Electricity_price_statistics. (Accessed 7 March 2025).

Fattahi, M., Govindan, K., Keyvanshokooh, E., 2018. A multi-stage stochastic program for supply chain network redesign problem with price-dependent uncertain demands. Comput. Oper. Res. 100, 314–332.

Gabrel, V., Murat, C., 2010. Robustness and duality in linear programming. J. Oper. Res. Soc. 61 (8), 1288–1296.

Galkin, P., Chen, D., Ward, C., 2023. Cost-Benefit Analysis for Petrochemical Projects. King Abdullah Petroleum Studies and Research Center.

Govindan, K., Fattahi, M., Keyvanshokooh, E., 2017. Supply chain network design under uncertainty: A comprehensive review and future research directions. European J. Oper. Res. 263 (1), 108–141.

Hasan, M.F., Boukouvala, F., First, E.L., Floudas, C.A., 2014. Nationwide, regional, and statewide CO_2 capture, utilization, and sequestration supply chain network optimization. Ind. Eng. Chem. Res. 53 (18), 7489–7506.

Hou, X., Jiang, Y., Wei, K., Jiang, C., Jen, T.-C., Yao, Y., Liu, X., Ma, J., Irvine, J.T., 2024. Syngas production from CO_2 and H_2O via solid-oxide electrolyzer cells: fundamentals, materials, degradation, operating conditions, and applications. Chem. Rev. 124 (8), 5119–5166.

IEA, 2021a. Transformation. Retrieved from hhttps://www.iea.org/reports/renewables-information-overview/transformation. (Accessed 7 March 2025).

IEA, 2021b. Policies database. Retrieved from https://www.iea.org/policies?country=Netherlands&topic=Fuels%20and%20technology%20innovation. (Accessed 5 January 2025).

IEA, 2023. Batteries and secure energy transitions. Retrieved from https://www.iea.org/reports/batteries-and-secure-energy-transitions. (Accessed 18 August 2024).

IEA Greenhouse Gas, 2023. Techno-economic assessment of electrochemical CO_2 conversion technologies. Retrieved from https://ieaghg.org/publications/techno-economic-assessment-of-electrochemical-co2-conversion-technologies/. (Accessed 10 January 2025).

IEAGHG Technical Report, 2023. 2023-03 techno-economic assessment of electrochemical CO_2 conversion technologies. Retrieved from https://ieaghg.org/publications/technical-reports/reports-list/9-technical-reports/1096-2023-03-techno-economic-assessment-of-electrochemical-co2-conversion-technologies. (Accessed 29 January 2024).

Institute for Sustainable Process Technology, 2023. Next level solid oxide electrolysis: Upscaling potential and techno-economical evaluation for 3 industrial use cases. Retrieved from https://ispt.eu/media/2023-SOE-public-report_ISPT.pdf. (Accessed 10 January 2025).

Institute for Sustainable Process Technology (ISPT), 2023. Next level solid oxide electrolysis. Retrieved from https://ispt.eu/media/20230508-FINAL-SOE-public-report-ISPT.pdf. (Accessed 13 December 2024).

Intratec, 2024. Cost of process water | Netherlands. Retrieved from https://www.intratec.us/products/industry-economics-worldwide/utility/process-water-netherlands. (Accessed 13 December 2024).

IRENA, 2024. Decarbonising hard-to-abate sectors with renewables: Perspectives for the G7. Retrieved from https://www.irena.org/Publications/2024/Apr/Decarbonising-hard-to-abate-sectors-with-renewables-Perspectives-for-the-G7. (Accessed 3 September 2024).

Jung, W., Jeong, J., Kim, J., Chang, D., 2020. Optimization of hybrid off-grid system consisting of renewables and Li-ion batteries. J. Power Sources 451, 227754.

Keyvanshokooh, E., Ryan, S.M., Kabir, E., 2016. Hybrid robust and stochastic optimization for closed-loop supply chain network design using accelerated Benders decomposition. European J. Oper. Res. 249 (1), 76–92.

Khosravani, H., Meshksar, M., Rahimpour, H.R., Rahimpour, M.R., 2023. Introduction to syngas products and applications. In: Advances in Synthesis Gas: Methods, Technologies and Applications. Elsevier, pp. 3–25.

Kojima, H., Nagasawa, K., Todoroki, N., Ito, Y., Matsui, T., Nakajima, R., 2023. Influence of renewable energy power fluctuations on water electrolysis for green hydrogen production. Int. J. Hydrog. Energy 48 (12), 4572–4593.

Li, N., Lukszo, Z., Schmitz, J., 2023a. An approach for sizing a PV–battery–electrolyzer–fuel cell energy system: A case study at a field lab. Renew. Sustain. Energy Rev. 181, 113308.

Li, Y., Zhou, S., Pan, G., 2023b. An effective optimisation method for coupled wind–hydrogen power generation systems considering scalability. Processes 11 (2), 343.

Linde Gas, 2024. Supply modes: Pipelines. Retrieved from https://www.linde-gas.com/what-we-offer/supply-modes/pipelines. (Accessed 25 June 2024).

McCormick, G.P., 1976. Computability of global solutions to factorable nonconvex programs: Part I–Convex underestimating problems. Math. Program. 10 (1), 147–175.

Melo, M.T., Nickel, S., Da Gama, F.S., 2006. Dynamic multi-commodity capacitated facility location: a mathematical modeling framework for strategic supply chain planning. Comput. Oper. Res. 33 (1), 181–208.

Melo, M.T., Nickel, S., Saldanha-Da-Gama, F., 2009. Facility location and supply chain management–A review. European J. Oper. Res. 196 (2), 401–412.

Metz, B., Davidson, O., De Coninck, H., Loos, M., Meyer, L., 2005. IPCC Special Report on Carbon Dioxide Capture and Storage. Cambridge University Press, Cambridge.

National Renewable Energy Laboratory, 2023. Utility-scale battery storage. Retrieved from https://atb.nrel.gov/electricity/2023/utility-scale_battery_storage. (Accessed 10 January 2025).

Nguyen, T.B., Leonzio, G., Zondervan, E., 2023. Supply chain optimization framework for CO_2 capture, utilization, and storage in Germany. Phys. Sci. Rev. 8 (8), 1685–1711.

Nishikawa, E., Islam, S., Sleep, S., Birss, V., Bergerson, J., 2023. Guiding research in electrochemical CO_2 conversion strategies through a systems-level perspective. Green Chem. 25 (1), 229–244.

Nowtricity, 2021. What is CO_2eq/Kwh and what does it mean? Retrieved from https://www.nowtricity.com/faq/. (Accessed 13 December 2024).

Nowtricity, 2024a. Historical data for Belgium. Retrieved from https://www.nowtricity.com/country/belgium/. (Accessed 13 December 2024).

Nowtricity, 2024b. Historical data for Netherlands. Retrieved from https://www.nowtricity.com/country/netherlands/. (Accessed 13 December 2024).

OpenAI, 2025. ChatGPT [Large language model].

Peng, P., Snyder, L.V., Lim, A., Liu, Z., 2011. Reliable logistics networks design with facility disruptions. Transp. Res. Part B: Methodol. 45 (8), 1190–1211.

Ramezani, M., Bashiri, M., Tavakkoli-Moghaddam, R., 2013. A robust design for a closed-loop supply chain network under an uncertain environment. Int. J. Adv. Manuf. Technol. 66, 825–843.

Sens, L., Neuling, U., Kaltschmitt, M., 2022. Capital expenditure and levelized cost of electricity of photovoltaic plants and wind turbines–Development by 2050. Renew. Energy 185, 525–537.

Solyalı, O., Cordeau, J.-F., Laporte, G., 2016. The impact of modeling on robust inventory management under demand uncertainty. Manag. Sci. 62 (4), 1188–1201.

Soyster, A.L., 1973. Convex programming with set-inclusive constraints and applications to inexact linear programming. Oper. Res. 21 (5), 1154–1157.

Statista, 2024a. Electricity demand in Luxembourg from 2000 to 2023, by origin. Retrieved from https://www.statista.com/statistics/1262851/electricity-demand-luxembourg/. (Accessed 13 December 2024).

Statista, 2024b. Annual electricity generation from solar photovoltaic in the Netherlands from 2012 to 2023. Retrieved from https://www.statista.com/statistics/497593/electricity-production-from-solar-in-netherlands/. (Accessed 7 December 2024).

Store & Go, 2019a. Analysis on future technology options and on techno-economic optimization. Retrieved from https://erig.eu/wp-content/uploads/2023/02/2019-07-04_STOREandGO_D7.7_accepted.pdf. (Accessed 13 December 2024).

Store & Go, 2019b. Innovative large-scale energy storage technologies and power-to-gas concepts after optimization. Retrieved from https://www.storeandgo.info/fileadmin/downloads/deliverables_2020/Update/2019-07-04_STOREandGO_D7.7_accepted.pdf. (Accessed 5 March 2025).

Tebibel, H., 2021. Methodology for multi-objective optimization of wind turbine/battery/electrolyzer system for decentralized clean hydrogen production using an adapted power management strategy for low wind speed conditions. Energy Convers. Manage. 238, 114125.

Timmerhaus, K.D., West, R.E., 2004. Plant Design and Economics for Chemical Engineers. McGraw-Hill.

Tsagkari, M., van de Poel, I., Pérez-Fortes, M., 2024. Sustainable design of multiscale CO_2 electrolysis: A value sensitive design-based approach. Energy Res. Soc. Sci. 116, 103671.

Vermeer, W., Mouli, G.R.C., Bauer, P., 2021. A comprehensive review on the characteristics and modeling of lithium-ion battery aging. IEEE Trans. Transp. Electr. 8 (2), 2205–2232.

Wiltink, T., Yska, S., Ramirez, A., Pérez-Fortes, M., 2023. Evaluation of centralized/decentralized configuration schemes of CO_2 electrochemical reduction-based supply chains. In: Computer Aided Chemical Engineering. Vol. 52, Elsevier, pp. 3417–3422.

Withanaarachchi, A.S., Nanayakkara, J., Pushpakumara, C., 2015. Delphi as a methodology for eliciting expert opinion–Important factors to be considered. Available At SSRN 2632765.

Wolff, M., Becker, T., Walther, G., 2023. Long-term design and analysis of renewable fuel supply chains–An integrated approach considering seasonal resource availability. European J. Oper. Res. 304 (2), 745–762.

Zhang, S., Liu, L., Zhang, L., Zhuang, Y., Du, J., 2018. An optimization model for carbon capture utilization and storage supply chain: A case study in Northeastern China. Appl. Energy 231, 194–206.

Zhang, S., Zhuang, Y., Tao, R., Liu, L., Zhang, L., Du, J., 2020. Multi-objective optimization for the deployment of carbon capture utilization and storage supply chain considering economic and environmental performance. J. Clean. Prod. 270, 122481.

Zhao, K., Jia, C., Li, Z., Du, X., Wang, Y., Li, J., Yao, Z., Yao, J., 2023. Recent advances and future perspectives in carbon capture, transportation, utilization, and storage (CCTUS) technologies: A comprehensive review. Fuel 351, 128913.

Zokaee, S., Jabbarzadeh, A., Fahimnia, B., Sadjadi, S.J., 2017. Robust supply chain network design: An optimization model with real world application. Ann. Oper. Res. 257, 15–44.

Van der Zwaan, B., Schoots, K., Rivera-Tinoco, R., Verbong, G., 2011. The cost of pipelining climate change mitigation: An overview of the economics of CH_4, CO_2 and h_2 transportation. Appl. Energy 88 (11), 3821–3831.